Distribution Agreement

In presenting this thesis or dissertation as a partial fulfillment of the requirements for an advanced degree from Emory University, I hereby grant to Emory University and its agents the non-exclusive license to archive, make accessible, and display my thesis or dissertation in whole or in part in all forms of media, now or hereafter known, including display on the world wide web. I understand that I may select some access restrictions as part of the online submission of this thesis or dissertation. I retain all ownership rights to the copy right of the thesis or dissertation. I also retain the right to use in future works (such as articles or books) all or part of this thesis or dissertation.

Signature:

_____ _____

Brandy Elizabeth Wade Date

Ubiquitin Targeting and Differential Accumulation of Mutant Huntingtin

By

Brandy Elizabeth Wade
Doctor of Philosophy

Graduate Division of Biological and Biomedical Sciences
Genetics and Molecular Biology

_____
Xiao-Jiang Li, M.D., Ph.D.
Advisor

_____
Gary Bassell, Ph.D.
Committee Member

_____
Joseph Cubells, Ph.D.
Committee Member

_____
Andrew Escayg, Ph.D.
Committee Member

_____
Zixu Mao, Ph.D.
Committee Member

Accepted:

_____
Lisa A. Tedesco, Ph.D.
Dean of the James T. Laney School of Graduate Studies

_____
Date

Ubiquitin Targeting and Differential Accumulation of Mutant Huntingtin

By

Brandy Elizabeth Wade
B.S., University of Texas Pan American, 2008

Advisor: Xiao-Jiang Li, M.D., Ph.D.

An *abstract* of
A dissertation submitted to the Faculty of the
James T. Laney School of Graduate Studies of Emory University
in partial fulfillment of the requirements for the degree of
Doctor of Philosophy

Graduate Division of Biological and Biomedical Sciences
Genetics and Molecular Biology

2014

Abstract

Ubiquitin Targeting and Differential Accumulation of Mutant Huntingtin

By
Brandy Elizabeth Wade

Huntington's disease (HD) is a rare and fatal neurodegenerative disease caused by expansion of a polyglutamine (polyQ) tract in the N-terminus of the gene encoding the huntingtin (Htt) protein. PolyQ expansion of 37 or more causes neurodegeneration that is particularly severe in the striatum and cortex compared to other brain regions. Expansion of the polyQ tract causes the protein to misfold and selectively accumulate in an age dependent manner. Htt is expressed throughout the entire body; however, it only accumulates in the brain. The mechanism underlying the selective accumulation and toxicity observed in HD is unknown. In this study we observed that in HD knock-in mice mHtt expression is higher in the brain. However, expression of mHtt at the same level via injection of viral vectors results in greater accumulation in the striatum than in the muscle. Development of an in vitro degradation assay revealed that mHtt is more stable in the brain. Striatal and cortex tissues also promote the formation of high molecular weight (HMW) mHtt. Protein stability is tightly linked to ubiquitination, a process requiring the catalytic activity of three enzymes to. Ubiquitination requires an E1, E2 and E3 to activate, and subsequently link an ubiquitin (Ub) moiety to a target protein. Using a pyrazone compound, PYR41, which targets and inactivates the Ubiquitin E1 enzyme (Ube1) we were able to observe an increase in formation of HMW mHtt complexes even in tissues that are relatively unaffected in HD. Importantly, Ube1 protein levels are lower in brain tissues than peripheral tissues and decline in the nucleus with age. This is correlated with the increase accumulation of mHtt that is observed in the brain with aging. These finding suggest that decreased Ub targeting may contribute to differences in stability between tissues which leads to the preferential accumulation of toxic forms of mHtt in the brain. Thus, we have discovered a novel mechanism that contributes to the age related accumulation of mHtt and the selective toxicity that characterizes HD.

Ubiquitin Targeting and Differential Accumulation of Mutant Huntingtin

By

Brandy Elizabeth Wade
B.S., University of Texas Pan American, 2008

Advisor: Xiao-Jiang Li, M.D., Ph.D.

A *dissertation* submitted to the Faculty of the
James T. Laney School of Graduate Studies of Emory University
in partial fulfillment of the requirements for the degree of
Doctor of Philosophy

Graduate Division of Biological and Biomedical Sciences
Genetics and Molecular Biology

2014

ACKNOWLEDGEMENTS

I would like to thank my advisor, Xiao-Jiang Li for his support during my time as a graduate student in his lab. He challenged me and helped shape my work into the best it could be. I would also like to thank Shi-hua Li for her assistance and advice in technical aspects of experiments. I would also like to thank my committee members who were always willing and able to help me look at my work in a new way to help me solve difficult experimental problems. I also want to thank my amazing friends for their help in coping with the stress of graduate school. Not only were they always there with a cold beer and a friendly ear, they were always there to boost my confidence when I needed it the most. I especially want to thank Nicole Umberger and Matthew Randolph for making the day to day work of graduate school more bearable. They always knew when I needed chocolate, ice cream or hugs. My family also deserves a shout out for their love and commitment to my dream. They have supported me through all of the ups and downs I have experienced. My mother especially, comforted me and supported me through all of the craziness of both graduate school life and everyday life. Of all the people who have supported me, Louis Kiphen, my now husband deserves the most credit. He moved to Atlanta with me so that I could pursue this dream. He has been a constant source of love, pizza, coffee and support. Thank you, Louis Kiphen, for your love and support. I could not have done this without you.

Table of Contents

Chapter 1

General Introduction

1.1 Poly Glutamine Diseases

Poly glutamine (PolyQ) repeat expansion is known to cause nine inheritable neurodegenerative disorders including Huntington's disease (HD), Spinocerebellar Ataxia (Weiss et al., 2012) 1, 2, 3, 6, 7, 17, Spinal and bulbar muscular atrophy (SBMA) and Dentatorubral-pallidoluysian atrophy (DRPLA). Each of these diseases is caused by expansion of a variable length poly-glutamine stretch in different proteins. While these proteins serve different functions, are found in different cellular compartments, affect different brain regions and share no homology aside from the polyQ tract, the polyQ diseases share several features.

Expansion of the PolyQ tract in each of the disease proteins results in a neurodegenerative phenotype, which is restricted to specific brain regions (**Table 1.1**). Another commonality shared by the Poly Q expansion disorders is the ability of the disease protein to form proteinaceous aggregates and neuronal nuclear inclusions (NI) in a poly Q length dependant manner. The role of these protein aggregates is heavily debated in the field. Protein aggregates were originally thought to be the source of toxicity in polyQ diseases. This was supported by the advent of the R6/2 transgenic mouse lines which expressed exon 1 of human mutant huntingtin protein (mhtt) with 144 CAG repeats (Mangiarini et al., 1996). The R6/2 transgenic line developed a rapid onset neurological phenotype and these animals also developed pronounced neuronal nuclear inclusions (Davies et al., 1997). However, it was also shown that aggregate formation did not correlate with neurodegeneration in post mortem tissues from HD patients (Li et al., 2001). Discrepancies such as these raise the question of what role aggregates

really play. Given the shared ability of proteins containing an expanded polyQ tract to aggregate, it is likely that large poly glutamine tracts aggregate on their own and the differences observed in the disease phenotypes are due to protein context differences (Ordway et al., 1997).

Aside from SBMA, which is an X-linked recessive disorder, polyQ expansion causes dominant mutations. This means that only one copy of the mutated protein is required to cause the disease and a single functional copy of the protein is not sufficient to overcome the effect of the mutant protein. Mice transgenic for the mutant huntingtin gene still express wild type Htt but still develop a phenotype (Gray et al., 2008; Hodgson et al., 1999; Mangiarini et al., 1996). In polyQ diseases expansion of the glutamine tract results in gain of function of the disease protein via aberrant interaction with other proteins. For example, the mutated huntingtin protein (mhtt) disrupts transcriptional activity through aberrant interactions with transcriptional activator Sp1 and coactivator TAFII130 (Dunah et al., 2002). In 1995, the first huntingtin associated protein-1 (HAP1) (Li et al., 1995) was identified. HAP1 was later shown to be involved in huntingtin-mediated axonal transport (Gauthier et al., 2004) via interaction with $p150^{GLUED}$. Increased interaction between mHtt, HAP1 and $p150^{GLUED}$ resulted in decreased interaction of HAP1/ $p150^{GLUED}$ with microtubules and a subsequent decrease in axonal transport.

Loss of function has also been implicated in polyQ diseases. In HD reduced levels of BDNF transcript and protein in HD models and post mortem tissues from HD patients (Zuccato et al., 2001) was shown to be caused by a reduced interaction between mHtt and repressor element-1 silencing

transcription factor/neuron restrictive silencing element (RE1/NRSE)(Zuccato et al., 2003). Under normal conditions, wild type htt would sequester RE1/NRSE in the cytoplasm, preventing it from silencing brain derived neurotropic factor (BDNF) gene transcription. However, in HD, the expanded htt protein has a reduced ability to sequester RE1/NRSE, allowing it to accumulate in the nucleus and reduce transcription of BDNF. Since BDNF is an important factor in the survival and support of neurons. A decrease in BDNF has long been thought to play a major role in the loss of striatal neurons that characterizes HD.

1.2 Huntington's Disease

Huntington's disease is a rare but fatal neurodegenerative disease, affecting approximately 5-10 individuals per 100,000 in worldwide populations (Driver-Dunckley E, 2007) and 1 in 10,000 in populations of European ancestry (Harper, 1992). Symptoms and characteristics of Huntington's disease were very well described in 1872 by the disease namesake, George Huntington. The most prominent symptom of HD is chorea, though subtle psychological changes, such as depression and other personality changes may precede development of physical symptoms (Martin and Gusella, 1986). Typically HD manifests in middle age, though HD can manifest in juveniles with CAG tracts longer than 60. Juvenile HD is characterized by rapid, early onset and severe symptoms including rigidity and seizures, more widespread neurodegeneration and aggregate formation (Nance and Myers, 2001).

The disease mutation responsible for HD was mapped to a large gene, *IT15*, on chromosome 4 (Group, 1993). The huntingtin gene (htt) is large,

~350kd, and contains a variable length polyQ tract (11-37) in exon 1 of the gene. In HD patients the htt gene contains a polyQ tract of 37 or more CAGs, with the polyQ length being inversely correlated with age of onset (Duyao et al., 1993). Juvenile HD patients usually have a CAG of more than 60. The mutant length polyQ tract is highly unstable and can expand and retract between generations (Duyao et al., 1993; Group, 1993).

To distinguish between loss of function and gain of function models of HD, the mouse homologue (*hdh*) was inactivated by several groups (Duyao et al., 1995; Nasir et al., 1995; Zeitlin et al., 1995). Homozygosity for the null allele was embryonic lethal demonstrating that the huntingtin protein is functionally necessary for early development. Despite its crucial role in development the exact function of the htt protein remains unknown. It is thought to act as a scaffolding protein involved in neuronal trafficking. Htt interacts with huntingtin associated protein-1 (HAP1)(Gauthier et al., 2004; Li et al., 1995), which binds to subunits of the microtubule proteins kinesin and dyenin in the axonal transport of vesicles (Li et al., 1998; McGuire et al., 2006).

Despite the ubiquitous expression of the wild type and mutant htt proteins (Li et al., 1993; Sharp et al., 1995; Strong et al., 1993), HD is characterized by selective neurodegeneration beginning in the striatum and spreading to other regions of the basal ganglia as well as the cortex in later stages of the disease (de la Monte et al., 1988; Vonsattel et al., 1985) . The Medium Spiny Neurons (MSNs) of the striatum are particularly affected though the reason is unknown. Evidence that Ubiquitin Proteasome System (UPS) activity is reduced in neurons compared to glia (Tydlacka et al., 2008) suggests that reduced UPS activity makes neurons

more sensitive to misfolded mhtt protein than glia. The expanded polyQ tract in mhtt protein leads to protein misfolding (Perutz, 1994) and subsequent aggregation (Zhou et al., 2003). While a pathological hallmark of HD, their role is not well characterized.

1.3 Huntingtin Protein and N-Terminal Fragments of Huntingtin Protein

The huntingtin protein (htt) is a large protein that is ubiquitously expressed and generally found in the cytoplasm. The N-terminus of htt contains a 17 amino acid region that is important for its localization and contains a nuclear export signal. This region is followed by the polyQ tract and a short poly proline tract. The C-terminal section of htt is composed almost entirely of HEAT repeats (**Figure 1.1**)(Andrade and Bork, 1995; Li et al., 2006). As mentioned previously, the expanded polyQ tract is able to form nuclear inclusions (Cooper et al., 1998; DiFiglia et al., 1997; Lunkes et al., 2002; Wang et al., 2008a; Zhou et al., 2003). These inclusions are composed of N-terminal fragments of mHtt that are able to enter the nucleus. These fragments become trapped in the nucleus due to decreased nuclear export through reduced interaction with the nuclear pore protein, translocated promoter region (Tpr) (Cornett et al., 2005). Proteolytic cleavage of polyQ disease proteins is also important for aggregate formation in other poly Q expansion diseases such as SCA-3, SBMA and DRPLA (Haacke et al., 2007; Schilling et al., 1999b; Wellington et al., 1998). N-terminal mHtt fragments (N-mHtt) are particularly important since they have been shown to be sufficient to cause cellular dysfunction in cell lines and cultured striatal neurons and an HD

like neurological phenotype *in vivo* (Cooper et al., 1998; Mangiarini et al., 1996; Ratovitski et al., 2007; Saudou et al., 1998). Interestingly, these N-mHtt fragments are also sufficient to form aggregates both *in vitro* and *in vivo* (Cooper et al., 1998; Davies et al., 1997).

Many N-terminal fragments of mutant huntingtin protein have been identified (**Figure 1.1**). Huntingtin protein containing both an expanded and non-expanded polyQ tract is cleaved into smaller fragments by proteases. Full length htt is cleaved by caspases 2 and 3 at amino acids 513 and 552 as well as caspase 6 at amino acid 586 (Wellington et al., 1998; Wellington et al., 2000). Interestingly, both mutant htt and non-expanded htt are cleaved by caspases (Kim et al., 2001; Wellington et al., 2002), indicating that caspase cleavage may not be a toxic event. However, the accumulation of the caspase cleavage product may lead to neurodegeneration. Htt protein is also cleaved by calpains at amino acids 469 and 536 (Gafni et al., 2004) in a polyQ dependent manner (Gafni and Ellerby, 2002). The htt protein is also cleaved by matrix metalloproteases at amino acid 402 (Miller et al., 2010). Aspartic endopeptidases generate two small mHtt fragments termed Cp-A and Cp-B that have been mapped to amino acids 102-114 and 146-214 respectively (Lunkes et al., 2002). Suppressing the formation of these small N-mHtt fragments has been shown to reduce toxicity (Gafni et al., 2004; Miller et al., 2010; Wellington et al., 2000). An exon 1 fragment of mHtt has been shown to be formed through aberrant splicing events (Sathasivam et al., 2013).

1.4 Proteostatic disruption in Huntington's disease

HD is often considered a proteostatic disease since accumulation and aggregation of a misfolded protein is a hallmark of the disease. There are two main mechanisms of degrading misfolded proteins to be recycled by the cell, autophagy and the ubiquitin proteasome system (UPS). These two cellular clearance mechanisms are linked by the ubiquitin targeting system or ubiquitination. Ubiquitination is a three step process (**Figure 1.2**) in which an ubiquitin moiety is covalently added to a target protein on a lysine residue. Ubiquitin (Ub) is a small, 8.5 kD, regulatory protein that is highly conserved across species (Goldstein et al., 1975) and contains 7 internal lysine (K) resides (6, 11, 27, 29, 33, 48, 63) through which the Ub moiety can be linked to target proteins. Ub molecules can be added as monomers (mono-ubiquitination) or as chains (poly-ubiquitination- PolyUb). Different types of ubiquitination target proteins to different fates. The first step in ubiquitination involves a ubiquitin-activating enzyme (E1) which activates Ub in an ATP dependent reaction. The E1 then transfers the active Ub to the active site on an ubiquitin-conjugating enzyme (E2). This E2-Ub complex then binds to an ubiquitin-ligase (E3) which interacts directly with target proteins and ligates the active Ub to the target protein. Ub chains of 4 or more are degradation signal. K48 and K63 Ub linkages are the most well understood types of poly-Ub. K63 Ub linkage has been linked to targeting to autophagy (Tan et al., 2008) while K48 Ub linkage is linked to the UPS.

Mutant Htt aggregates are ubiquitinated *in vivo*. Researchers suggested that misfolded mHtt is recognized as "abnormal" and subsequently ubiquitinated

causing the formation of aggregates. Instead, evidence in transgenic and knock-in models of HD as well as HD patients, suggests that ubiquitin is recruited to aggregates after they are formed (DiFiglia et al., 1997; Gong et al., 2012; Kuemmerle et al., 1999). Full length human mHtt (Kalchman et al., 1996) and N-term mHtt fragments are known to be ubiquitinated (Bhat et al., 2014), though this ubiquitination is not likely to be causative in the formation of aggregates since not all aggregates are ubiquitinated, suggesting that ubiquitination occurs after their formation. Recent evidence shows that both full length and N-term mHtt are preferentially ubiquitinated by K63 linked Ub chains (Bhat et al., 2014).

The htt protein can also be sumoyolated. The SUMO protein is functionally distinct from Ub, though it is bound to proteins in three step process similar to that of Ub. Ub plays a role in degradation, while SUMO tagging is biologically linked to increased protein stability. Exon 1 mHtt can be sumoyolated to increase soluble mHtt stability and decrease aggregation. In a fly model of HD, increased SUMO activity leads to increased neurodegeneration while increased Ub activity decreases neurodegeneration (Steffan et al., 2004).

Autophagy

Autophagy is responsible for turnover of organelles, misfolded proteins and aggregated proteins and occurs in the cytoplasm. First, misfolded proteins are targeted for autophagy by the binding of p62 to ubiquitinated proteins. This recruits other autophagic proteins to form a double membrane vesicle, called an autophagosome, which sequesters cytosol. The autophagosome then fuses with a lysosome, forming an autolysosome. Lysosomal enzymes then degrade the proteins within the compartment (**Figure 1.3**). Controversy has surrounded the

impact of mHtt on autophagy; however, knock down of autophagy components *Atg5* and *Atg7* in mice causes neurodegeneration and accumulation of ubiquitin positive inclusions in the absence of any other disease causing genes (Hara et al., 2006; Komatsu et al., 2006). *Atg 5* deficiency is also known to increase mHtt aggregation in HD striatal cell lines (Lee et al., 2012). Chemically suppressing autophagy through the use of Bafilomycin A1 (BfA1) or 3-methyladenin (3-MA) increases mHtt aggregation and increases cell death (Ravikumar et al., 2002). Reciprocally, autophagic induction can reduce neurodegeneration in HD fly and mouse models (Ravikumar et al., 2004).

Several regulators of autophagy are disrupted in HD. p62 is upregulated in HD mouse and patient striatal tissue (Lee et al., 2012) while Beclin-1, the human ortholog of yeast autophagy-related gene *Atg6*, is increased in HD cell lines (Martinez-Vicente et al., 2010). Beclin-1 is also known to decrease with age in the normal human brain (Shibata et al., 2006). Contradictory research showed a decrease in proteolysis in HD cells but no observable change in the clearance of autophagosomes, also called autophagic flux. An increase in the number and size of autophagosomes was also observed. Curiously, these autophagosomes appeared to be empty upon close inspection by electro-microspcopy. These same researchers observed an increase in the interaction between mHtt and p62 (Martinez-Vicente et al., 2010). Combined, these data suggest that in HD, mHtt aberrantly interacts with p62, disrupting autophagy targeting and triggering the formation of autophagosomes with fewer or no cytosolic components. These autophagosomes undergo normal fusion with lysosomes; however there is

reduced protein turnover within autolysosomes due to the reduced cargo load within the original autophagosome.

The Proteasome

The proteasome is another target for poly-Ub proteins. K48 poly-Ub is the canonical signal for protein degradation via the proteasome. The 26S proteasome is a protein complex composed of the 19S regulatory element and the 20S core. The 19S element recognizes and binds to poly-Ub proteins, releases the ubiquitin moieties, unfolds the degradation substrate and then shuttles it into the 20S core where the protein is degraded (**Figure 1.4**)(Chau et al., 1989). The 20S core is a cylindrical complex composed of 4 stacks of heteroheptameric ring complexes. The two internal rings have trypsin-like, chymotrypsin-like, and peptidylglutamyl peptide hydrolase activities which are responsible for substrate degradation. The proteasome can be found in both the cytoplasm and the nucleus and is mainly responsible for turnover of short-lived, misfolded and damaged proteins (Kerscher et al., 2006; Li and Li, 2011; Lim and Lim, 2011).

Like autophagy, UPS impairment is a contentious topic in HD. Two models of proteasome impairment have been proposed to explain age dependent accumulation and toxicity in HD. The first model proposed that proteasome impairment is caused by sequestration of proteasome subunits in mHtt aggregates. This was suggested due to the observation that proteasome subunits colocalized with polyQ containing aggregates (DiFiglia et al., 1997). However, this model was proven incorrect since cells expressing exon 1 of mHtt develop proteasome impairment regardless of mHtt aggregates formation. This same

study found that mHtt aggregate formation did not significantly alter proteasome subunit distribution (Bennett et al., 2005).

The second model of proteasome impairment suggests that the expanded polyQ tract may be inefficiently or slowly degraded by the proteasome, subsequently clogging the proteasome pore. It is well documented that inhibition of the proteasome is toxic to striatal cells in a dose dependent manner (Mitra et al., 2009) and that chemical inhibition of proteasome activity causes an increase in mHtt aggregates *in vitro* (Zhou et al., 2003) and *in vivo* (Li et al., 2010). Green-fluorescent protein ubiquitin (GFPu) reporter proteins (Bence et al., 2001) allowed detailed dissection of proteasome activity in HD models. Several studies observed a decrease in proteasome activity in HD models (Bence et al., 2001; Bennett et al., 2005; Jana et al., 2001; Venkatraman et al., 2004). Compared to wild type littermates, R6/2 transgenic HD mice show an accumulation of poly-Ub proteins (Bennett et al., 2007). Conflicting reports observed no difference in proteasome activity between controls and HD models (Bett et al., 2009; Maynard et al., 2009; Ortega et al., 2010) while still others observed an increase in proteasome activity in the striatum and cortex of HD knock-in mice (Diaz-Hernandez et al., 2003). While no difference was observed in total cell extract, impaired proteasome activity was found in the synapses of R6/2 and HD knock-in mice (Wang et al., 2008b). In support of this model, aggregates in the neuropil are not ubiquitinated as frequently as those the nucleus (Gutekunst et al., 1999; Li et al., 1999). Some studies suggest that endogenous expression of mHtt does not impair proteasome activity but acute expression is sufficient to reduce proteasome activity (Ortega et al., 2010), though it is relieved by formation of

mHtt aggregates (Mitra et al., 2009). The mechanism of proteasome impairment in HD is not fully understood, though evidence supports an age dependent decline in proteasome activity regardless of HD status (Tonoki et al., 2009; Tydlacka et al., 2008; Zhou et al., 2003).

1.5 Aggregation of Expanded Poly Glutamine Protein

N-terminal fragments of mHtt and other proteins containing expanded polyQ tracts become misfolded and can subsequently form aggregates (**Figure 1.5**). Glutamine repeats have been shown to form β- sheets and when expanded, polyQ tracts form polar zippers (Perutz, 1995), which can self associate to form proteinacous aggregates. Indeed, insertion of an expanded polyQ tract into a non-disease causing gene, hypoxanthine phosphoribosyltransferase (Hprt), is sufficient to cause a late onset neurological phenotype in mice. The resulting Hprt polyQ protein is capable of forming polyQ containing protein inclusions (Ordway et al., 1997).

In HD, polyQ containing aggregates are formed in a polyQ length dependent manner (Li and Li, 1998; Scherzinger et al., 1997) and in a Htt fragment length dependent manner (Hackam et al., 1998). Large protein aggregates, or inclusions, are found in the neuropil and the nucleus of neurons in HD mouse models (Davies et al., 1997; Hodgson et al., 1999; Schilling et al., 1999a) and HD patient brain tissue (DiFiglia et al., 1997). These aggregates increase in size, number and distribution with age and are considered a hallmark of Huntington's disease.

Early on, htt aggregates were thought to be pathogenic; however, aggregates are not well correlated with affected regions of the brain. Htt inclusions are found more prominently in the cortex than the striatum and are observed more frequently in neurons that are spared degeneration (Gutekunst et al., 1999; Kuemmerle et al., 1999). While suppression of nuclear localization of mHtt protein has been shown to suppress neurodegeneration, inclusion formation was not associated with mHtt induced apoptosis (Saudou et al., 1998). Disruption of aggregate formation actually lead to an increase in mHtt induced cell death (Saudou et al., 1998). These discrepancies make polyQ protein aggregation a source of great controversy in the field. These discrepancies initiated the search for another toxic culprit in Huntington's disease.

Mutant huntingtin protein can form several types of aggregate precursors, termed oligomers or protofibrils. These oligomers form in a polyQ length dependant manner prior to aggregate formation (Legleiter et al., 2010). Like aggregates, these oligomers are composed of small N-term mHtt fragments (Poirier et al., 2002). Oligomers are formed both *in vitro* and *in vivo* (Sathasivam, 2010) and can be found in post mortem HD patient brain samples but not in HD patient fibroblast lines (Marcellin et al., 2012). These oligomers have been shown to decrease with the age dependent formation of insoluble protein aggregates. In a drosophila model of HD, the molecular chaperones Hsp 40 and Hsp 70 were shown to reduce mHtt toxicity and neurodegeneration without altering the incidence of nuclear inclusions (Kazemi-Esfarjani and Benzer, 2000; Warrick et al., 1999). Later this activity was shown to be through

their interaction with soluble monomers of mHtt to reduce formation of an aggregate precursor (Lotz et al., 2010; Wacker et al., 2004).

1.6 Hypothesis

Considering the tissue specific nature of mHtt toxicity and aggregation despite the widespread expression of mHtt, I hypothesized that peripheral tissues modulate mHtt expression and toxicity differently than the brain. This dissertation explores differences in tissue specific processing and accumulation of mHtt protein. I also aim to identify factors that may contribute to accumulation of mHtt with age in the nucleus of neurons in the striatum. I found that not only is expression of mHtt different in different tissue, mHtt is more stable in the brain than in peripheral tissues. I also saw that brain tissues are more capable of forming high molecular weight Htt complexes (HMW) than peripheral tissues that are unaffected in HD. I discovered lower levels of Ubiquitin activating enzyme 1 (UBE1) in the brain compared to peripheral tissues as well as a decrease in nuclear UBE1 with age in the brain. These findings help to explain the tissue specific nature of HD as well as the age dependent disease progression.

Table 1.1. PolyQ Diseases

Poly Q Disease	Normal CAG	Mutant CAG	Disease Protein	Protein Function	Affected Brain Region (Cell Type)
Dentatorubral-pallidoluysian atrophy (DRPLA)	7-34	49-88	Atrophin-1	Transcriptional regulation	Cerebellum, (Purkinji Cells)
Huntington's Disease (HD)	6-34	36-121	Huntingtin	Scaffolding protein, axonal transport	Striatum (Medium Spiny Neurons)
Spinocerebellar Ataxia 1 (SCA1)	6-39	40-81	Ataxin-1	Transcriptional co-repressor	Cerebellum, (Purkinji Cells)
Spinocerebellar Ataxia 2 (SCA2)	15-24	32-200	Ataxin-2	RNA Metabolism	Cerebellum, (Purkinji Cells)
Spinocerebellar Ataxia 3 (SCA3/MJD)	12-39	61-84	Ataxin-3	Poly-Ubiquitin editing enzyme	Spinal cord and Brain Stem
Spinocerebellar Ataxia 6 (SCA6)	4-19	10-33	CACNA1A	Voltage gated Ca^{2+} Channel Subunit	Cerebellum, (Purkinji Cells)
Spinocerebellar Ataxia 7 (SCA7)	4-35	37-306	Ataxin-7	Transcriptional Repressor	Cerebellum, (Purkinji Cells)
Spinocerebellar Ataxia 17 (SCA17)	25-42	47-63	TATA Binding Protein (TBP)	Transcription Factor	Cerebellum
Spinal and bulbar muscular atrophy (SBMA)	9-36	38-62	Androgen Receptor	Transcriptional Activation	Lower Motor Neurons

Figure 1.1

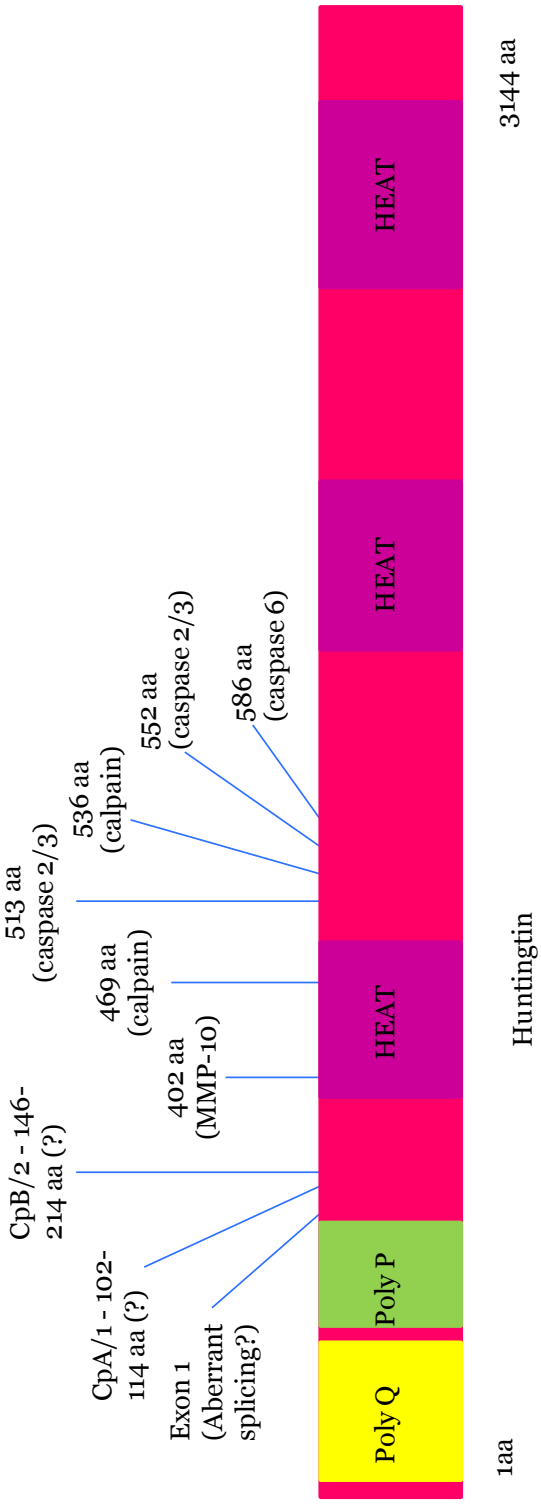
CpB/2 - 146-
214 aa (?)
CpA/1 - 102-
114 aa (?)
Exon 1
(Aberrant
splicing?)
513 aa
(caspase 2/3)
469 aa
(calpain)
402 aa
(MMP-10)
536 aa
(calpain)
552 aa
(caspase 2/3)
586 aa
(caspase 6)
Poly Q
Poly P
HEAT
HEAT
HEAT
1aa
Huntingtin
3144 aa

Figure 1.1. Huntingtin Protein

The huntingtin protein (htt) is a 3144 amino acid protein. Its molecular weight is approximately 350kD. In the N terminal region it contains a poly glutamine tract (yellow) which, when expanded past 37 CAG's can cause Huntington's disease. The poly glutamine tract is followed immediately by a poly proline (green) tract. In the C- terminus, the protein contains several HEAT repeats (purple). Htt is suspected of acting as a scaffolding protein. The protein can be cleaved into several small fragments (blue lines indicate approximate cleavage sites).

Figure 1.2

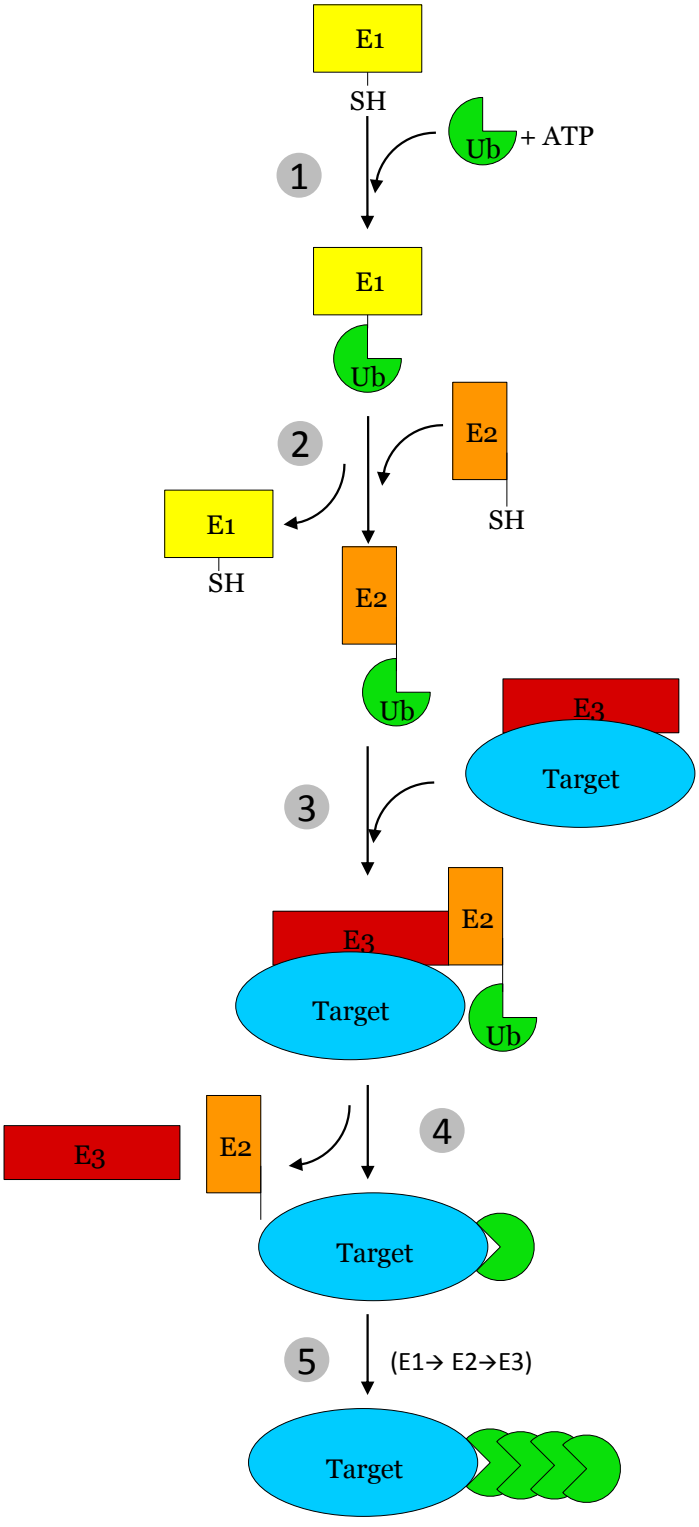
E1
SH
Ub
+ ATP
1
E1
Ub
E2
2
E1
SH
SH
E2
Ub
E3
Target
3
E3
E2
Target
Ub
E3
E2
4
Target
5
(E1→ E2→E3)
Target

Figure 1.2. Ubiquitination Cascade

1) Ubiquitin-activating enzyme (E1- in yellow) binds inactive ubiquitin and, in an ATP dependent reaction, activates the Ubiquitin moiety.

2) E1-Ub is bound by an ubiquitin-conjugating enzyme (E2- in orange) and the active ubiquitin is transferred from the E1 to the E2.

3) An ubiquitin-ligase enzyme(E3- in red) binds to the E2-ubiquitin complex. E3 can be bound to the target prior to complexing with the E2 (depicted) or the E3 can bind the E2 prior to binding the target.

4) The E3 facilitates the transfer of the active ubiquitin to the target substrate and the complex is dissociated.

5) Steps 1-4 are repeated, with active ubiquitin being attached to a lysine on the first ubiquitin on the target protein. This is repeated to extend the ubiquitin chain.

Figure 1.3

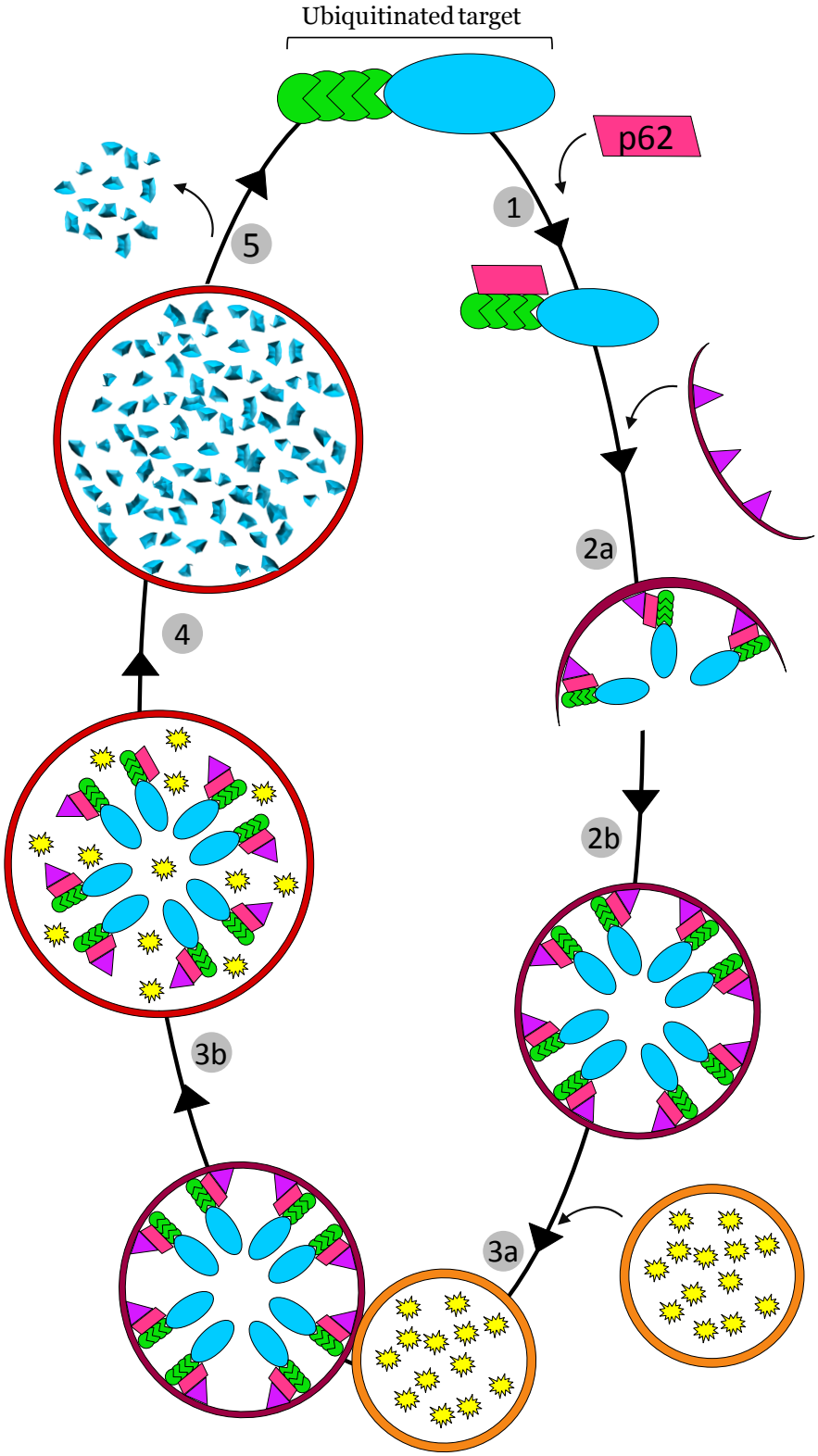

Figure 1.3. Autophagy Pathway

1) The ubiquitin (in green) chain attached to the target protein (teal oval) can be bound by p62 (pink rhombus).

2a) A double membrane structure (burgundy semi-circle) called the phagophore dotted with LC3 (purple triangles) is recruited by p62.

2b) The phagophore envagenates to surround cytosolic components including the target protein. This is called an autophagosome.

3a) The lysosome (orange circle) filled with acid hydrolase enzymes (in yellow) is recruited to the autophagosome.

3b) The lysosome fuses with the autophagosome, releasing it's contents. This structure is called an autolysosome.

4) The contents of the autolysosome are degraded into peptides by lysosomal enzymes.

5) The autolysosome dissociates and releases the degraded contents into the cytoplasm.

Figure 1.4

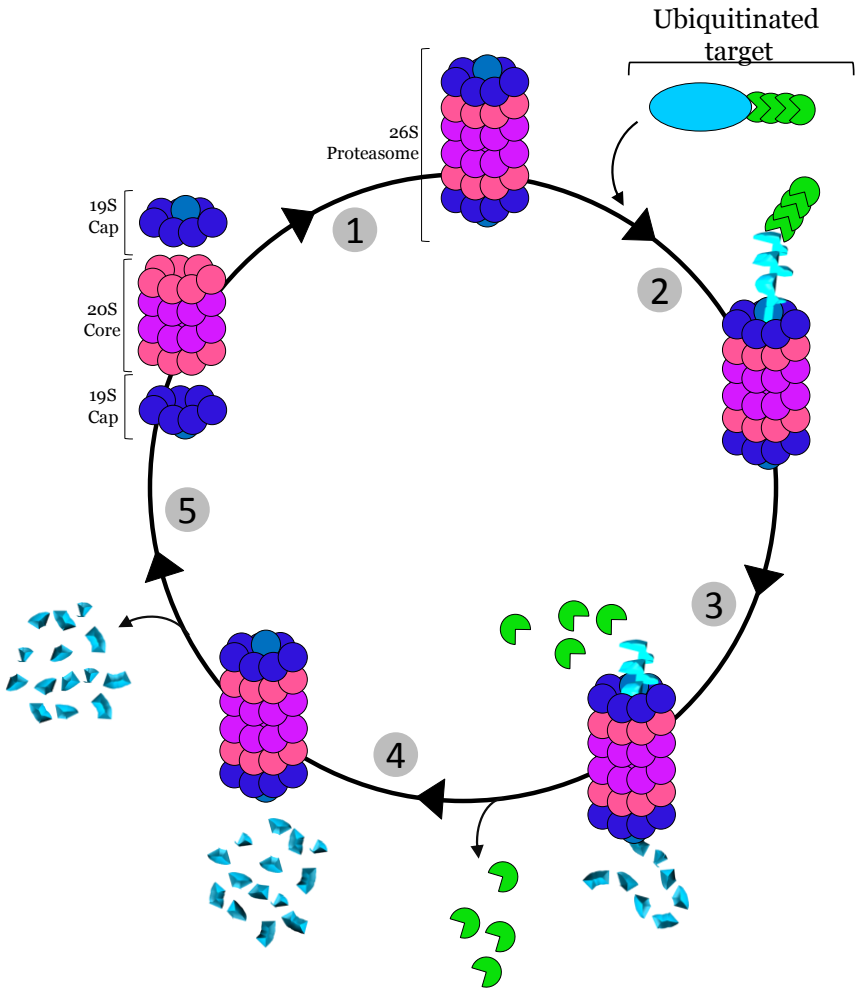
Ubiquitinated target
26S Proteasome
19S Cap
20S Core
19S Cap
1
2
3
4
5

Figure 1.4. The Proteasome Degradation Pathway

1) The 19S cap and 20S core associate to form the 26S proteasome.

2) Ubiquitinated (green) target is recruited to the proteasome and unfolded by the 19S cap and the unfolded protein is shuttled into the 20S core through the pore.

3) The cap removes the ubiquitin chain as the protein is degraded into small peptides inside the 20S core.

4) The fully degraded protein is released into the cytoplasm as small peptides.

5) The proteasome dissociates.

Figure 1.5

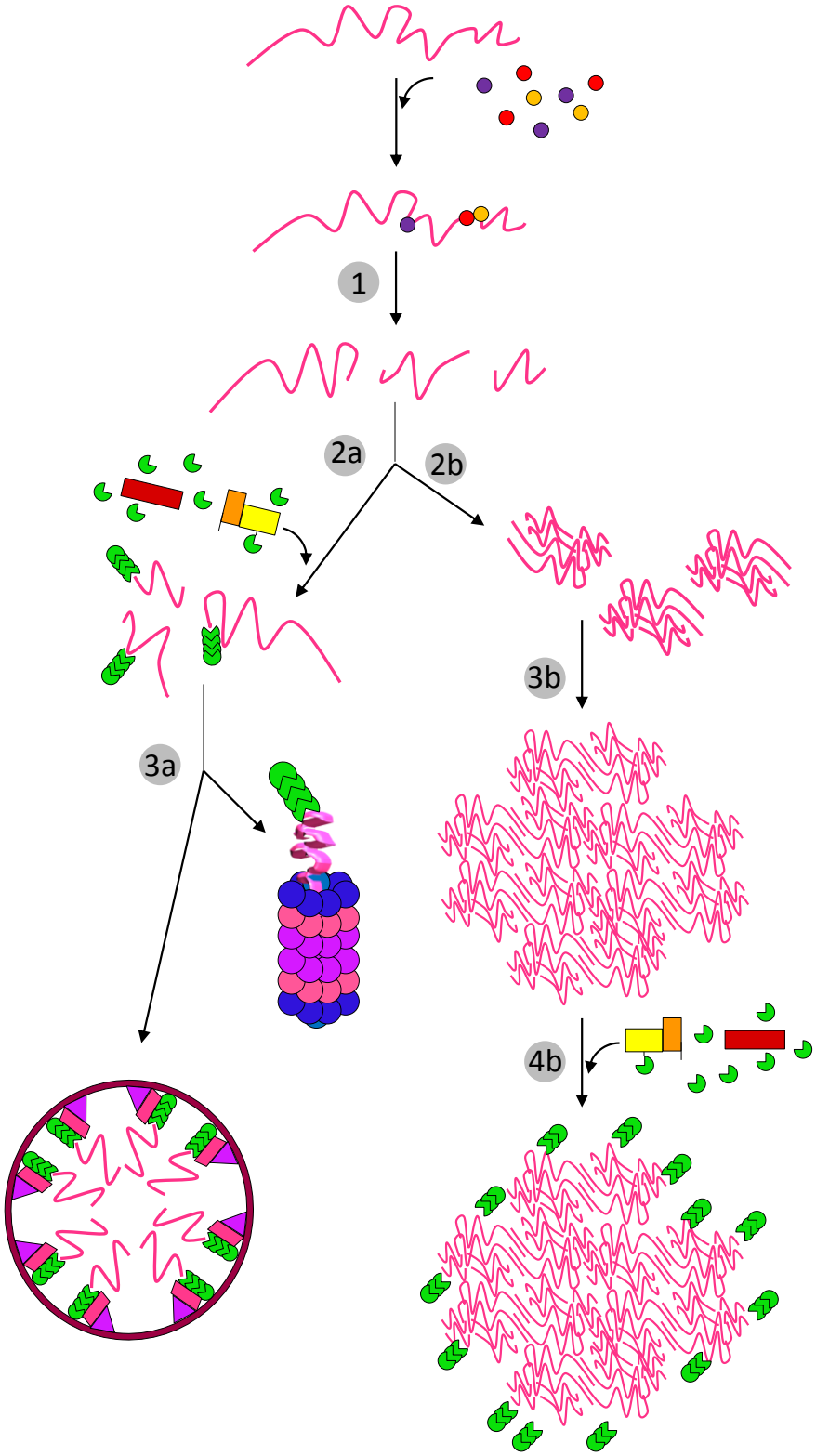

Figure 1.5. Huntingtin protein lifecycle

1) Huntingtin protein (htt- in pink) is cleaved into fragments by various protease (indicated by red, purple and orange dots). These fragments can then undergo one of two fates.

2a) Huntingtin fragments can remain soluble and can then be ubiquitinated by the ubiquitin cascade (yellow, orange and red boxes indicate ubiquitination enzymes, green pan men indicate free ubiquitin). For more information about the Ubiquitin cascade, see Figure 1.2.

3a) Ubiquitinated htt fragments can then be degraded by either autophagy (left branch) or the proteasome (right branch). For more description of these pathways see Figures 1.3 and 1.4.

2b) Mutant huntingtin fragments can oligomerize to form soluble polymers of protein.

3b) Oligomerized mHtt protein can eventually form large insoluble aggregates.

4b) Large mHtt aggregates can then be ubiquitinated to form ubiquitin positive inclusion bodies.

Chapter 2

Materials and Methods

This chapter was published in part as: Brandy E Wade, Chuan-En Wang, Sen Yan, Kavita Bhat, Brenda Huang, Shihua Li, Xiao-Jiang Li (2014) *The Journal of Neuroscience* June 34(25):8411– 8422. Xiao-Jiang Li and Shihua Li helped with the experimental design. Xiao-Jiang Li played a key role in the preparation of the manuscript.

2.1. Animals

Animal procedures were approved by the Institutional Animal Care and Use Committee (IACUC) of Emory University. Full-length mHtt CAG140Q (HD KI) mice were kindly provided by Dr. Michael Levine of UCLA (Hickey et al., 2008) and were maintained at the Emory University Animal facility in accordance with IACUC guidelines. For stereotaxic Injection of virus and behavioral studies, 3 female and 2 male mice per group were used. For the remainder of the experiments, both sexes were used.

2.2 Plasmids and antibodies

PRK vectors expressing 1-212 (N212) or 1-508 (N508) N-terminal Htt fragments containing 23Q (Mangiarini et al.) or 120/150Q (mutant) were generated previously (Havel et al., 2011; Li and Li, 1998). The lentiviral vectors were constructed by adding a digested F2A-ECFP fragment to the C-terminus of Htt in the PRK vector. The htt-F2A-ECFP DNA fragment was then excised and ligated into the pFUW viral backbone for viral production. The final virus was packaged and amplified by the Emory University Viral Vector Core and expresses Htt and ECFP under the same promoter and in the same cells in which F2A self-cleavage can separate Htt and ECFP proteins.

2.3 Antibodies and Western Blotting

The mouse anti-Htt (mEM48) was produced previously in our laboratory (Wang et al., 2008a; Zhou et al., 2003). Primary antibodies used for immunoblotting and immunoprecipitation assays were as follow: mouse anti-mHtt (mEM48), mouse 1C2 (Millipore, Temecula, CA), mouse anti-tubulin

(Sigma-Aldrich), GAPDH (Ambion), P4D1 1:1000 (Cell Signaling), GAPDH 1:80,000 (Millipore), eIFα 1:10,000 (Santa Cruz), Vinculin 1:10,000 (Sigma), 1C2 1:10,000 (Millipore), TFIIB 1:1000 (Santa Cruz Biotech), SNAP25 1:20,000 (Sigma) K63 specific Apu3 1:1000 (Millipore), K48 linked Ubiq 1:1000 (Cell Signaling) and SUMO-2/3 1:125 (MLB International).

Whole brains from WT and HD KI mice were dissected to isolate the cortex, striatum, and cerebellum. Peripheral tissues (kidney, liver, heart and calf muscle) were also dissected out. The tissues were homogenized for 25 strokes in ice-cold homogenization buffer (10 nM Na2HPO4, 5 mM EDTA, 5 mM EGTA, 0.02% NaN3) containing 1:100 protease inhibitor cocktail (Thermo Scientific: Pierce) and 100 μM PMSF. For Western blotting, samples were boiled for 5 min in SDS/BME protein loading dye and run at 50 mA for 125 min on 4-12% Tris-Glycine gels purchased from Invitrogen (Cat #EC60385). Proteins were transferred to a nitrocellulose membrane for 80 min at 105V in Tris-Glycine buffer. After blocking for 30 min in a 5% dry milk in 1X PBS, blots were probed with mEM48 or other primary antibodies diluted in 3%BSA in PBS at 4° overnight. The western blots were developed using the ECL Prime Chemiluminescence kit (GE Health Care/Amersham Biosciences).

2.4 Immunohistochemistry

Six month old HD KI mice were anesthetized and perfused intracardially for 30 sec with phosphate-buffered saline (PBS, pH 7.2) followed by 4% paraformaldehyde in 0.1 M phosphate buffer (PB) at pH 7.2. Brains were dissected out and cryoprotected in 30% sucrose at 4°C. Thin (40 μm) sections

were obtained using a freezing microtome. Free-floating sections were preblocked in 4% normal goat serum in PBS, 0.1% Triton X, and incubated with EM48 antibody at 4°C for 48 h. The rabbit EM48 (1:2000) immunoreactive product was visualized with the Avidin–Biotin Complex kit (Vector ABC Elite, Burlingame, CA, USA).

2.5 Subcellular Fractionation

For subcellular fractionation, whole brain cortex was collected from 4-, 8-, and 12-month-old HD CAG140 knock-in mice, and fractions (P1, P3 and S3) were prepared using the method of Sharp *et al.* (Sharp et al., 1995). Tissues were homogenized with 10 strokes of a 2ml glass Dounce tissue grinder with the glass B pestle in ice cold 0.32 M sucrose in 4mM HEPES (pH 7.4) with protease inhibitors and PMSF. Lysates were centrifuged at 1000xg for 10 min at 4°C to separate the P1 and S1. The P1 was resuspended and washed again (1000xg for 10 min at 4°C) to yield the nuclear fraction which is suspended in 100µl homogenization buffer. S1 was centrifuged at 17,600xg for 20 min at 4°C. The S2 was then centrifuged at 100,000xg for 1 h 15 min in a swinging bucket rotor to separate the P3 (synaptosome fraction) and the S3 (soluble cytoplasm fraction). The P3 was resuspended in 200-300µl buffer depending on pellet size. Protein samples were prepared as described earlier.

2.6 Formic Acid Solubilization

For formic acid solubilization of mHtt aggregates, cortex, cerebellum, and striatum were dissected out from a 7-month-old heterozygous HD CAG140 knock-in mouse. Formic acid solubilized aggregates were obtained following

procedures previously outlined (Landles et al., 2010; Lunkes et al., 2002; Zhou et al., 2003). Tissues were homogenized with 10 strokes of a Teflon pestle in a 2 mL glass Potter-Elvehjem tissue grinder in ice-cold buffer (50 mM Tris-HCl pH 8.8, 100 mM NaCl, 5mM $MgCl_2$, 1 mM EDTA ph 8.0, 0.5% NP40, plus protease inhibitors). Lysates were centrifuged 800xg at 4°C to fractionate into crude nuclear and cytoplasmic fractions. Freshly made SDS buffer (500 µl, 2% SDS, 5% BME, 15% glycerol, protease inhibitors) was added to the crude nuclear pellet and boiled for 10 min. The boiled nuclear pellet was sonicated for 20 s at 5 mA with 0.6 sec on and 0.5 sec off. The sonicated sample was split into two tubes for treatment with and without formic acid then centrifuged for 15 min at 16,200xg at room temperature. The pellet (insoluble aggregates) was incubated in 100% formic acid with shaking (350 rpm) at 37°C for 1 h. The formic acid was removed by vacufuge (30°C, 2 h), and then the sample was reduced in freshly made 1M Tris Base with protease inhibitors.

2.7 Cell cultures

Human embryonic kidney 293 (HEK 293) cells (ATCC, Manassa, VA), HD stable HEK293 cell lines fHtt-23Q, and fHtt-120Q were established previously (Zhou et al., 2003) and cultured in DMEM/F12 (Invitrogen, Grand Island, NY) containing 10% (v/v) fetal bovine serum, 100 units/ml of penicillin, 100 µg/ml streptomycin (Invitrogen), and 250 µg/µl fungizone amphotericin B. Cells were maintained at 37°C in 5% CO_2 incubators. Stable cell lines were selected using 500 µg/ml hygromycin (Invitrogen). For transient transfections, cells were plated at 75% confluency and transfected with 1 µg (for 12-well plates), 2 µg (for 6-well

plates), or 4 μg (for 10-cm plates) of plasmid DNA using Lipofectamine 2000 (Invitrogen) in serum-free DMEM (Gibco) for 5 h. After 5 hours the transfections media was removed and cells were grown in the media described above.

2.8 *In vitro* degradation assay (IVDA)

Htt HEK 293 cells stably expressing transfected full-length Htt were grown to confluence in a 10-cm plate. Cells were washed in the plate then lysed in cold assay buffer (25 mM Tris-HCl, pH 7.6, 10 mM MgCl, 100 ug/ml purified rabbit creatine kinase, 50 mM phosphocreatine, 1 mM ATP - added at use). Wild-type mice were sacrificed and tissues (striatum, cerebellum, cortex, kidney, liver, heart, muscle) were rapidly collected and homogenized at 1g/1ml in cold assay buffer using 20 strokes of a 2ml glass dounce hand homogenizer using the glass B pestle. Both cell lysates and tissues were centrifuged 500xg at 4°C for 5 min to pellet unbroken tissues and membranes. The supernatant was collected and stored on ice while protein concentrations were determined using a BCA Protein Assay Kit (Thermo Scientific). Both tissue and cell lysates were prepared at 170 μg protein/500 μl assay buffer, and the appropriate number of 200μl aliquots was prepared. The samples containing both cell and tissue lysates were mixed in a 1 to 1 ratio (i.e. 200 μl cell lysates + 200 μl tissue lysates). The control samples contained equal volumes of tissue or cell lysates and assay buffer. The samples were incubated in a pre-heated shaking incubator at 37°C with 300RPM shaking for 0, 8, or 16 h. The reaction was stopped by the addition of protease inhibitors, PMFS, and protein loading dye. The samples were immediately stored at -80°C until use.

For inhibiting the proteasome and E1 enzymes, IVDA samples were prepared as described previously (WT tissue and HEK 293 cell lysate) or from HD CAG140 KI mouse tissue (Menalled et al., 2003) which were collected and homogenized in cold assay buffer (25 mM Tris-HCl, pH 7.6, 10 mM MgCl, 100 ug/ml purified rabbit creatine kinase, 50 mM phosphocreatine, 2 mM ATP). Tissue lysates were prepared as in the IVDA and diluted to 170 µg protein/500 µl assay buffer, and the appropriate number of aliquots was prepared. 50 µM MG132 or 50 µM PYR41 (Yang et al., 2007) were added to appropriate tubes. The reaction was incubated and stopped as described above.

2. 9 qRT-PCR and RT-PCR

In preparation for RNA extraction, all surfaces and tools were cleaned and treated with RNAse Away to prevent DNA contamination and to eliminate RNase. Total RNA was isolated from the HD CAG140 KI mouse cortex, striatum, cerebellum, muscle, kidney, liver, and heart using the RNeasy Lipid Tissue Mini Kit (Qiagen Inc.), and RT reactions were performed with 2 µg of total RNA as described previously (Wang et al., 2008a). Tissue was chopped using a new RNase AWAY treated razor then homogenized in 1 ml QiAzol Lysis Reagent in a 2 ml eppendorf tube using a battery operated tissue grinder with a disposable sterile plastic adaptor. The sample was then incubated for 5 min at room temperature (RT) followed by the addition of chloroform and vigorous shaking. This was incubated at RT for 3 min then centrifuged at 12,000xg for 15 min at 4°C. The upper layer (the aqueous phase) was transferred to a new tube and mixed by vortexing with 600 µl 70% Ethanol. 700 µl of the sample was then

transferred to an RNeasy Mini spin column in a collection tube and centrifuged at 8,000xg for 15 sec at RT and the flow through was discarded. This step was repeated until all of the sample had been used. 700 µl Rw1 Buffer was then added to the RNeasy spin column. The sample was then capped and centrifuged at 8,000xg for 15 sec. The flow through was then discarded. Next, 500 µl of RPE buffer was added to the column and centrifuged at 8,000xg for 15 sec then the flow through was discarded. This was performed again with a centrifugation step for 2 min. The column was then moved to a new 1.5 ml collection tube and 30 µl of RNase-free water was added to the column. The capped column was then centrifuged at 8,000xg for 1 min. This was repeated. The RNA concentration of the eluate was determined using a Nano Drop 2000 (Thermo Scientific).

First-strand cDNA synthesis was performed using the SuperScript III First Strand Synthesis System for RT-PCR (Invitrogen). 1.5 µg of RNA was transferred to a sterile 0.2 ml PCR tube. 1 µg of oligo(Shaid et al.)$_{20}$, 1 µl random hexamers, 1 µl 10mM dNTP mix and DEPC-treated water were added to the RNA to a volume of 10 µl. This mixture was gently centrifuged then incubated at 65°C for 5 min then on ice for 1 min. Next, the following mixture was prepared in a new tube in this order: 2 µl 10X RT buffer, 4µl 25mM $MgCl_2$, 2 µl 0.1 M DTT, 1 µl RNase OUT (40 U/µl) and 1 µl SuperScript III RT (200 U/µl). This mixture was then added to the RNA primer mixture and briefly centrifuged to mix. The mixture was then incubated as follows: 10 min at 25°C, 50 min at 50°C, 5 min at 85°C. The reaction was then placed on ice for 1 min. 1 µl RNase H was then added and the sample was then incubated for 20 min at 37°C. The final sample was aliquoted in 10 µl samples then stored at -20°C until use.

qRT PCR reactions were performed using SYBR Select Master Mix (Applied Biosystems). The following was prepared in a 96 well blue skirted optical plate in triplicate for each sample (3 using htt primers, 3 using GAPDH primers): 10 µl SYBR Select Master Mix, 1 µl forward primer, 1 µl reverse primer, 5 µl cDNA, 3 µl RNase-free water. The optical plate was then sealed with an optical adhesive cover and centrifuged gently. The plate was read using a Realplex Mastercycler (eppendorf). The htt levels were normalized to GAPDH levels using the formula: $R=2^{\wedge(C_{htt} - C_{gapdh})}$.

RT-PCR was performed using: 2.5 µl TaKaRa Buffer, 2 µl dNTPs, 0.2 µl TaKaRa Taq, 1 µl each Htt primers, 0.25 µl each GAPDH primers, 1 µl cDNA, 16.8 µl ddH_2O. The following primers were used: primers specific for mouse and human htt were HD1S (forward) 5'-ATGGCGACCCTGGAAAAGCT-3' and HD40A (reverse) 5'-TGCTGCTGGAAGGACTTGAG-3'; GAPDH mRNA was detected using GAPDH 958S (forward) 5'- AACTTTGTCAAGCTCATTTCCTGGT -3' and GAPDH 1032A (reverse) 5'- GGTTTCTTACTCCTTGGAGGCCATG -3' .The following PCR cycles was used:

1) 94°C 3 min
2) 94°C 45 sec
3) 64°C 45 sec
4) 72°C 60 s (30 cycles for qRT-PCR, 28 cycles for RT-PCR)
5) 72°C 10 min.

The RT-PCR products were then separated on a 4% agarose gel by electrophoresis at 120V for 50 min.

2.10 Viral Injection: Stereotaxic and muscle injections

Three-month-old wild-type mice (C3H) were anesthetized using 0.39 ml/20 g 2.5% Avertin. During surgery respiratory rate and skin coloration were monitored visually to ensure animals safety. The animals were injected in either the right hemisphere or bilaterally with 1.5 µl ($1.08x10^{12}$) lentivirus per side with the following coordinates set from the bregma: 2 mm lateral, 0.6 mm anterior, -3.3 mm ventral. The flow rate was 200 nanoliters/min and there was a 3-min delay before the needle was slowly removed (1.1 mm every 7 min). The animals were monitored daily and administered the analgesic ketoprofen (Fort Dodge Animal Health) at 2 mg/ml for 3 days post-surgery.

For muscle injection, mice were anesthetized using 0.39 ml/20 g 2.5% Avertin (Alfa Aesar), and 1.5 µl virus was diluted to 50 µl with sterile 1XPBS and injected into the calf muscle using a 100-µl Hamilton syringe with a 27-g disposable needle. The needle was inserted almost to the ankle and removed slowly while dispensing the diluted virus. Analgesics were administered as described.

2.11 Rotarod assay

Animals were tested on a Rotamex Rotarod (Columbus Instruments) 3 times per day on 3 consecutive days. After a constant slow rotation, the speed was increased gradually over the course of 10 min from 5 rev/sec to 30 rev/sec. Data from all 3 days were averaged and used for comparison of each group (n=5).

2.12 Densitometry and Statistical Analysis

Immunoblot signals were quantified using either ImageJ or UN-SCAN-IT. We used the same size section on the blots for quantification to ensure accuracy between sections. All data have been quantified as a ratio of protein to a loading control (vinculin or elF5α) and then normalized within the experiment to facilitate comparison between experiments.

Quantifications of western blots were obtained using ImageJ and UN-SCAN-IT. The repeated-measures (RM) two-way ANOVA and two-way ANOVA were performed using Prism 6.0 (GraphPad). An alpha of 0.05 or less was considered significant. Where exact p values were not generated by Prism, they were obtained using the =TDIST(x, DF, t) function in Excel where x is the t value, DF is the degrees of freedom (these are provided in Prism) and t is the number of tails to test. Two tails were used since the change observed could be either higher or lower than the normal distribution. An example is =TDIST(0.03317, 45, 2) for a p-value of 0.9737. Bonferroni correction was used in the case where multiple testing occurred. The uncorrected p-value was multiplied by the number of tests. An example where 4 comparisons are made is (0.9737)*4= 3.8947.

Chapter 3

Ubiquitin-activating enzyme activity contributes to differential accumulation of mutant huntingtin in brain and peripheral tissues

This chapter presents work published as: Brandy E Wade, Chuan-En Wang, Sen Yan, Kavita Bhat, Brenda Huang, Shihua Li, Xiao-Jiang Li (2014) *The Journal of Neuroscience* June 34(25):8411– 8422. Brandy Wade performed all of the experiments in this chapter with the exception of the immunohistochemistry of cortex, striatum and kidney, which was performed by Chuan-En Wang (Figure 3.3). Xiao-Jiang Li and Shihua Li helped with the experimental design. Xiao-Jiang Li played a key role in the preparation of the manuscript.

3.1 Abstract

Huntington's disease (HD) belongs to a family of neurodegenerative diseases caused by misfolded proteins and shares the pathological hallmark of selective accumulation of misfolded proteins in neuronal cells. Polyglutamine expansion in the HD protein, huntingtin (htt), causes selective neurodegeneration that is more severe in the striatum and cortex than other brain regions, but the mechanism behind this selectivity is unknown. Here we report that in HD knock-in mice, the expression levels of mutant Htt (mHtt) are higher in brain tissues than in peripheral tissues. However, expression of N-terminal mutant Htt via stereotaxic injection of viral vectors in mice also results in greater accumulation of mHtt in the striatum than in muscle. We developed an *in vitro* assay that revealed extracts from the striatum and cortex promote the formation of high molecular weight (HMW) mHtt compared with the relatively unaffected cerebellar and peripheral tissue extracts. Inhibition of ubiquitin-activating enzyme E1 (Ube1) increased the levels of HMW mHtt in the relatively unaffected tissues. Importantly, the expression levels of Ube1 are lower in brain tissues than peripheral tissues and decline in the nuclear fraction with age, which is correlated with the increased accumulation of mHtt in the brain and neuronal nuclei during aging. Our findings suggest that decreased targeting of misfolded Htt to the proteasome for degradation via Ube1 may underlie the preferential accumulation of toxic forms of mHtt in the brain and its selective neurodegeneration.

3.2 Introduction

Huntington's disease (HD) is an autosomal dominant neurodegenerative disease caused by an expansion of the polyglutamine (polyQ) tract in the huntingtin protein (Htt). This progressive neurodegenerative disease is characterized by the loss of neurons, which is most pronounced in the striatum and cerebral cortex, resulting in symptoms such as chorea, dystonia, depression, cognitive deficits, and in the late stage, death (Landles and Bates, 2004). A pathological hallmark of the disease is formation of cytoplasmic and intranuclear aggregates or inclusions that consist of small N-terminal fragments of mutant Htt (mHtt) (DiFiglia et al., 1997; Gutekunst et al., 1999). There are transgenic mouse models that expresses N-terminal fragments of mutant proteins, but develop more severe phenotypes (Davies et al., 1997; Schilling et al., 1999b; Xu et al., 2013) than HD models expressing full-length mHtt (Gray et al., 2008; Slow et al., 2003), suggesting that smaller N-terminal mHtt is more toxic than longer mHtt fragments. However, how N-terminal Htt fragments accumulate in the brain and cause HD pathogenesis remains to be investigated.

Although both wild-type and mHtt are ubiquitously expressed throughout the body, there is no correlation between the expression of Htt and the brain regions most affected by the disease (Fusco et al., 1999; Gutekunst et al., 1999; Kuemmerle et al., 1999; Li et al., 1993). The role of mHtt aggregates and inclusions is also controversial. mHtt can form several types of aggregate precursors, termed oligomers or protofibrils in a polyQ length-dependent manner (Legleiter et al., 2010)and can be found in brain tissues from HD mouse models (Sathasivam et al., 2010). The role, if any, of these mHtt oligomers in HD

toxicity is still unclear, though evidence suggests that there are multimeric pools of oligomerized mHtt that can form aggregates with age (Marcellin et al., 2012). Since aggregate formation does not correlate well with HD toxicity, oligomerized mHtt, rather than aggregated mHtt, is suspected of being the toxic intermediary.

Despite the controversial role of mHtt aggregates, that these aggregates are ubiquitinated is evident (Davies et al., 1997; DiFiglia et al., 1997; Gutekunst et al., 1999). Protein ubiquitination is initiated by ubiquitin-activating enzymes (E1), which then pass the ubiquitinated proteins to E2 conjugating enzymes and E3 ligases for targeting to the proteasome for degradation (Schulman and Harper, 2009). Protein ubiquitination and degradation are involved in a variety of cellular functions (Kerscher et al., 2006) as well as in removing misfolded and toxic proteins in a variety of neurodegenerative diseases (Lim and Lim, 2011; Liu et al., 2007; Tan et al., 2008). However, we know very little about how ubiquitination contributes to the preferential accumulation of mutant proteins in neuronal cells. In the current study, we observed that the differential formation of high molecular weight (HMW) mHtt and aggregates in the brain and peripheral tissues is modulated by E1–E2–E3 targeting activity and that ubiquitin-activating enzyme expression correlates with the differential accumulation of mHtt. Our findings offer new insight into the preferential accumulation of mHtt and its selective neurodegeneration.

3.3 Results

mHtt is more stable in brain than peripheral tissues

Mutant Htt (mHtt) is ubiquitously expressed; however, HD is characterized by neurological symptoms and degeneration in specific regions of the brain. This selective neurodegeneration has been a long-standing issue for researchers to address since it does not correlate directly with Htt expression levels or observed protein aggregation (Fusco et al., 1999; Gutekunst et al., 1999; Kuemmerle et al., 1999; Li et al., 1993). We first compared mHtt expression levels in brain and peripheral tissues in a HD CAG140Q knock-in mouse model, which expresses full-length mHtt under the control of the endogenous mouse Htt promoter and shows the progressive phenotypic development and formation of mHtt aggregates (Hickey et al., 2008; Menalled et al., 2003). Western blotting revealed a different array of mHtt fragments in each tissue from a 7-month-old HD KI mouse (**Fig. 3.1A**). Full-length (FL) mHtt (open arrow) appears to be less stable in peripheral tissues as we were unable to detect it by immunoblotting with either antibody to N-terminal Htt (mEM48) or antibody to expanded polyQ repeats (1C2). Fewer N-terminal mHtt fragments were seen in the peripheral tissues than in brain regions, suggesting that mHtt proteolysis may be different between brain and peripheral tissues. We then performed quantitative RT-PCR to quantify the levels of mHtt mRNA relative to GAPDH mRNA (**Fig. 3.1B**). There were higher levels of mHtt mRNA in all 3 brain regions than in the peripheral tissues, and mHtt is expressed at the lowest level in muscle. Immunohistochemistry with mEM48 revealed the accumulation and aggregation of mHtt in the cortex and striatum in 6-month-old HD KI mice, whereas there

was no obvious mHtt staining signal by mEM48 in the kidney (**Fig 3.1C**). Taken together, these data suggest there are differences in mRNA expression and the post-translational modification of mHtt in the brain and in peripheral tissues, which contribute to the differential accumulation, aggregation, and subsequent toxicity of mHtt N-terminal fragments.

We also purified Htt aggregates from the cortex, striatum, and cerebellum of HD KI mice at the age of 7 months using formic acid treatment to dissolve aggregates. We found that aggregates in different brain regions are formed by multiple N-terminal Htt fragments, which are the same in different brain regions (**Fig. 3.2**). Thus, the accumulation and aggregation of mHtt in different brain regions are unlikely to be due to intrinsic proteolysis differences of Htt, but rather result from tissue-specific factors that modulate the stability of these N-terminal Htt fragments.

mHtt is more stable and forms more high molecular weight (HMW) mHtt in tissues affected in HD *in vitro*

To better understand the early steps in the accumulation of mHtt, we designed an *in vitro* degradation assay (IVDA) that allows us to observe tissue-specific processing of mHtt by adding the same amount of mHtt to cellular lysates from different tissues. Full-length (FL) Htt proteins containing either 23Q or 120Q in transfected HEK293 cells (Zhou et al., 2003) were used as a source of Htt. Lysates from individual tissues (striatum, kidney, liver, heart, and skeletal muscle) in wild type mice were incubated with transfected Htt to test tissue-specific effects of modulation on Htt levels, stability, and aggregation. The tissue

lysates in a Tris buffer contained creatine kinase, phosphocreatine, and ATP (TCP-ATP buffer), which are necessary for energy-dependent protein post-translational modifications. After incubation for different times, the transfected Htt and lysates were subjected to western blotting (**Fig. 3.3A**). We then quantified the relative levels of mHtt on western blots by measuring its ratio to vinculin, a cytoskeletal protein that is stable even after a long incubation time. We found that FL-120Q (open arrow head) and N-terminal mHtt fragments are more stable in the striatal lysate than in the lysates from most peripheral tissues observed (**Fig 3.3B, 3.3C**). Two-way ANOVA using time and tissue type as separate variables revealed that the length of incubation time contributed the most to mHtt degradation (11.66% p=3.29E-6), whereas tissue type contributed 6.851% to the degradation (p=0.8137) across all groups. Multiple comparisons show that the decrease in mHtt reaches significance in the kidney (p=0.0351) and liver (p=0.0012) lysates at 16 hours, and in the muscle at both 8 and 16 hours (p=0.0003 and p=5.26E-7). However, the decrease in mHtt was not significant at either 8 or 16 hours in the striatal or heart lysates.

Noticeably, HMW mHtt (filled arrow head) was formed in the above *in vitro* assay (**Fig. 3.3B and 3.3C**). Two-way ANOVA suggests that tissue type contributed the most to oligomerized mHtt formation in the striatum compared to the periphery, accounting for 42.57% of the effect (p =0.0013). The incubation time accounted for only 8.139% of total variance (p=3.85E-7), with an interaction between the two factors (20.57%, p=2.70E-5). HMW mHtt formation is significantly higher at 8 and 16 hours incubation in the striatum compared to all four peripheral tissue lysates (8 h:p=6.10E-6,1.81E-6, 7.76E-7,7.33E-7; 16 h:

p=2.70E-6, 1.79E-7, 2.85E-7,3.30E-5). HMW mHtt formation did not reach significance in any of the peripheral tissues.

When comparing brain regions, the lysates from cortex and cerebellum yielded a significant decrease in mHtt at 16 hours incubation (p=0.0364 and p=0.0109), but there was no significant decrease with striatal lysates (**Fig. 3.3D and 3.3E**). This analysis suggests that mHtt is more stable *in vitro* with the striatal lysates than with the other tissue lysates. When comparing HMW mHtt in different brain regions (**Fig. 3.3D, 3.3E**), tissue type contributed 38.48% to the formation of HMW mHtt (p= 5.61E-5), while incubation time contributed 21.86% of the effect (p=5.99E-7), and 28.48% of the effect on oligomer formation is caused by an interaction between the two variables (p= 1.54E-5). Multiple comparison tests allowed us to see that more HMW mHtt was formed in the cortex and striatum lysates than in the cerebellum lysates at 16 hours incubation (p= 3.73E-9 and p=0.0301). No HMW mHtt was formed in control samples without brain tissue lysates (**Fig. 3.3D** first two lanes). These data show that *in vitro* the striatal tissue is less able to clear mHtt than the other tissues tested, and therefore more HMW mHtt is formed with the striatal lysates. This difference is consistent with the preferential accumulation of mHtt in the striatum of HD KI mice (Lin et al., 2001; Menalled et al., 2003) and the selective vulnerability of striatal neurons in HD.

N-terminal mHtt is more stable in the brain than in the muscle and causes motor dysfunction

Since HD mouse models suggest that small N-terminal fragments of mHtt are more toxic than full-length mHtt (Heng et al., 2008), we chose to examine the degradation and HMW mHtt formation of N-terminal mHtt fragments in the brain and peripheral tissues. Lentiviral constructs expressing N-terminal fragments of wild-type (Mangiarini et al.) and mHtt under the ubiquitin promoter were injected into the striatum and skeletal muscle. Muscle was chosen for comparison with brain because it, like neurons, is also a terminally differentiated tissue. The 3 viral vectors (**Fig. 3.4A**) used express a small N-terminal Htt fragment with 23Q (N212-23Q) or 120Q (N212-120Q), or a larger N-terminal mHtt fragment (N508-120Q). Viruses were injected into the striatum and the right calf muscle (n=3 per group) of 3-month-old WT mice. One month post-injection, the injected tissues were isolated for western blot analysis. All 3 transgenic Htt proteins were expressed clearly in the striatum of the injected mice, while we detected no or very little mHtt proteins (N212-120Q and N508-120Q) in the skeletal muscle by western blotting, despite a low level of normal N-terminal Htt (N212-23Q) (**Fig. 3.4B**). Importantly, the shorter N-terminal mHtt (N212-120Q) formed more aggregated htt than N508-120Q in the striatum, suggesting that the smaller N-terminal Htt fragment is more prone to misfolding (**Fig 3.4B**). These *in vivo* data agree with observations from our *in vitro* experiments that N-terminal mHtt is more stable in the brain than in the muscle.

Next we examined the *in vivo* toxicity of these mHtt fragments using the rotarod as a test of motor function. WT mice (n=5 per group) were injected

bilaterally with these viral Htt vectors in the striatum and used for longitudinal study. There was no significant difference in body weights among the 3 groups injected with viral vectors expressing different N-terminal Htt, though mice injected with mHtt show slightly less weight gain than mice injected with normal N-terminal Htt (**Fig. 3.4C**). One month post-injection, animals for the behavioral studies were trained for the rotarod test, and then examined at 6 weeks and once every 3 weeks afterward (**Fig. 3.4D**). Two-way ANOVA analysis revealed that Htt fragment contributed the most variance (20.09%, p=2.48E-21), and time, while accounting for only 3.76% of the effect, was still considered significant (p=1.04E-9). Mice injected with viral N212-120Q Htt performed worse than those with N508-120Q at all time points (6 w p=4.45E-12, 9 w p=1.44E-7, 12 w p=2.09E-13, 15 w p=4.29E-8, 18 w p=1.23E-7, 21 w p=2.71E-6, 24 w p=0.0002). This increased toxicity of N212-120Q is also consistent with the increased stability and aggregation of N212-120Q in the injected striatum seen by western blotting (**Fig. 3.4B**).

Ubiquitinated mHtt is increased in brain tissues

Given the differential toxicity and stability of N-terminal Htt, it was important to examine how striatal tissues modulate different fragments of mHtt. Thus, we incubated transfected Htt (N212-23Q, N212-120Q, and N508-120Q) with mouse striatal lysates. More HMW mHtt was formed by N212-120Q (**Fig. 3.5A**). Quantification by densitometry shows that oligomer formation by N212-120Q is significantly higher than HMW mHtt formation by N508-120Q (p=

0.0374) and N212-23Q (p= 0.0007) (**Fig. 3.5B**). This result suggests that HMW mHtt is formed readily by shorter N-terminal mHtt fragments.

Given the findings that N-terminal mHtt is more stable in the striatum and forms more HMW mHtt, we wanted to know whether there are differences in Htt ubiquitination in different brain regions and peripheral tissues using the IVDA. We compared total ubiquitin levels at 0 and 16 hours after incubation of full-length mHtt (FL-120Q) with cortex, striatum, and cerebellum tissue lysates. Western blots with anti-ubiquitin (P4D1) revealed that the incubation markedly increased protein ubiquitination in striatal lysates (**Fig. 3.5C**). Although the incubation also increase protein ubiquitination in brain tissue lysates without FL-120Q, adding FL-120Q markedly increased protein ubiquitination (left panel in **Fig. 3.5C**). Thus, this increase reflects mHtt ubiquitination in IVDA. Importantly, striatal lysates resulted in more ubiquitination than cortex and cerebellar lysates, and brain tissue lysates yielded greater ubiquitination then peripheral tissue lysates (**Fig. 3.5C**), which was also verified by quantitative analysis of the relative levels of ubiquitin on the blots (**Fig. 3.5D**). The peripheral tissues incubated with FL-120Q also showed a rise in total ubiquitin levels at 8 hours and then a decrease at 16 hours of incubation, though the ubiquitin levels are lower than those with brain tissue lysates. Two-way ANOVA showed that incubation time contributed the most to ubiquitination (32.25%, p=2.01E-5), and tissue type contributed 23.76% of the variance observed in all groups (p=0.0930, ns) (**Fig. 3.5D**). These differences can be interpreted in two ways: one is that ubiquitinated proteins could be cleared more

easily in the peripheral tissues, and the other is that more ubiquitinated proteins are generated in the brain than in the peripheral tissues.

Inhibiting ubiquitin-activating enzyme E1 promotes aggregate formation

To determine how differences in ubiquitination could contribute to the stability of mHtt, we inhibited ubiquitination using the drug PYR41, a cell-permeable pyrazone compound that is reported to irreversibly inhibit ubiquitin-activating enzyme E1 activity (Yang et al., 2007; Guan, 2012; Su, 2013; Xu, 2013). The IVDA was then performed using striatal and muscle lysates mixed with full-length mHtt (FL-120Q), with the addition of 50 μM PYR-41. For comparison, the UPS inhibitor MG132 (50 μM) was used to inhibit protein degradation by the proteasome. The blots were probed with Htt, K48 ubiquitin, K63 ubiquitin, and sumoylation antibodies. PYR41 caused greater generation of HMW mHtt in both the striatal and muscle mixtures than MG132 (**Fig 3.6A**). Quantification of densitometry verified that PYR41 treatment of both striatal and muscle tissues increased HMW mHtt ($p=0.0015$ and $p=0.0454$, respectively) to a greater extent than MG132 (**Fig. 3.6B**). To compare the levels of HMW mHtt formed by endogenous full-length mHtt in the striatum, cortex, and cerebellum, we used brain tissue lysates from HD KI mice to perform IVDA with MG132 or PYR41 treatment. The immunoblots were probed with anti-Htt and anti-ubiquitin to detect HMW mHtt and ubiquitinated proteins. Although total ubiquitinated proteins do not seem different between the drug treated samples and the control without drug treatment, both MG132 and PYR41 appear to increase the level of

HMW mHtt in the striatum and cortex (the upper panel in **Fig. 3.6C** and **Fig. 3.6D**). The lower level of HMW mHtt was seen with the cerebellar lysates than with the striatal and cortical lysates, which was also increased by PYR41. However, these increases are not statistically significance due to large variations in the limited number of experiments (n=3). Given that PYR41 blocks the degradation of ubiquitinated proteins by the ubiquitin-proteasome system (Yang et al., 2007); these results suggest that PYR41 may prevent the targeting of HMW mHtt to the proteasome, resulting in increased levels of HMW mHtt.

Ubiquitin-activating enzyme E1 is expressed at different levels in brain and peripheral tissues

Given the above *in vitro* data, it was important to investigate whether ubiquitin-activating enzyme E1 (Ube1) activity is correlated with the accumulation of mHtt in the brain. We therefore performed western blot analysis of brain and peripheral tissues with known differential levels of mHtt in HD KI mice (Fig. 1). Using an antibody to Ube1 and compared the ratio of Ube1 to eIF5α, a translational protein that is expressed in all of the types of cells used and is involved in translation elongation, cell cycle progression and actin dynamics (Si et al., 1996), we found that the expression levels of Ube1 are markedly lower in brain tissues than in peripheral tissues (**Fig. 3.7A**). The levels of Ube1 are also lower in the striatum (Ube1/ eIF5α: 1.2) and cortex (1.0) than in the cerebellum (1.4). There is no difference in Ube1 expression between HD KI and WT mouse tissues (**Fig. 3.7A**), suggesting that mHtt does not impair the expression of Ube1. If Ube1 expression is indeed critical for the levels of mHtt, we should also see low

levels of it in the nucleus and nerve terminals in which mHtt preferentially accumulates and forms aggregates. We next performed subcellular fractionation experiments using HD KI mice at 4, 8, and 12 months of age and found that the aggregated mHtt is increased in the nuclear and synaptosomal fractions from the older HD KI mice (**Fig. 3.7B**). More importantly, Ube1 levels are indeed lower in the nuclear and synaptosomal fractions than in the cytosolic fraction (**Fig. 3.7C**). Compared with the level of Ube1a at 4 months, the nuclear Ube1 level significantly declines with age (from 1.0 to 0.16), while synaptosomal Ube1 levels remain unchanged. This difference suggests that Ube1 activity is also important for the age-dependent accumulation of mHtt in neuronal nuclei, whereas other synaptic modulators may alter mHtt accumulation and aggregation in synapses during aging.

Based on the above findings and the fact that E1 enzymes target ubiquitinated proteins for degradation via the proteasome, we propose that differential E1 enzyme activities in different types of tissues and cells contribute to the differential accumulation of mHtt and its aggregation in neuronal cells. Reduced E1 enzyme activities may explain why mHtt preferentially accumulates in the brain and forms aggregates in the nucleus and synapses (**Fig. 3.8**).

3.4 Discussion

The selective neurodegeneration seen in a variety of neurodegenerative diseases has long been a puzzle. Understanding how mutant proteins selectively accumulate in the affected brain regions would help us understand this important and unresolved issue. In the present study, we developed a novel *in vitro* assay

that allows us to closely monitor the accumulation of mHtt in different tissues. This *in vitro* degradation assay (IVDA) demonstrates that mHtt is more stable in the brain than in peripheral tissues. Our findings here suggest that reduced targeting of misfolded mHtt to the proteasome for degradation may contribute to the preferential accumulation of mHtt in affected neurons and the selective neuronal vulnerability in HD.

We also found that mHtt mRNA expression is in general lower in the peripheral tissues than in brain regions. This difference could also help explain the increased toxicity of mHtt in neuronal cells. However, by expressing the same viral mHtt vectors in the striatum and muscles, we still saw more abundant accumulation of mHtt in the striatum. In addition, in different brain regions, such as the cortex and striatum, more mHtt mRNA is expressed in the cortex than in the striatum, though more and earlier accumulation of mHtt and aggregates are seen in the striatum in HD KI mice (Li et al., 2000a; Li et al., 2001; Lin et al., 2001). Thus, post-translational modification of mHtt appears to be important for the differential accumulation of misfolded forms of mHtt, at least in brain regions.

Using HD KI mice, we verified that aggregated htt is formed by small N-terminal mHtt. By injection of viral vectors expressing N-terminal mHtt into mice, we also confirmed that N-terminal mHtt fragments are toxic and can become misfolded and aggregated, causing motor dysfunction. The IVDA shows that tissues from the striatum, which is most severely affected in HD, promotes the formation of HMW mHtt by N-terminal mHtt to a greater extent than tissues from relatively unaffected regions and organs. At least two possibilities could

explain this phenomenon. One is that striatal tissue favors the generation of HMW or misfolded mHtt, and the other is that HMW Htt is more stable or less efficiently cleared in the striatum.

The ubiquitin-proteasome system plays a major role in clearing misfolded proteins, a process that involves multienzyme cascades. The first step of ubiquitin activation is mediated by the E1 enzymes that bind ATP and ubiquitin and catalyze ubiquitin C-terminal acyl-adenylation. The active ubiquitin is then passed by E1 enzymes to E2 conjugating enzymes and then E3 ubiquitin ligases, a reaction that is necessary for targeting of ubiquitinated proteins to the proteasome for degradation (Schulman and Harper, 2009). PYR41, a commercially available cell-permeable inhibitor, was found in a high-throughput screening of an E1–E2–E3 cascade (Yang et al., 2007); it does not affect ubiquitination of proteins, but blocks the degradation of ubiquitinated proteins by the proteasome (Yang et al., 2007), giving us a useful tool to examine the targeting of ubiquitinated proteins to the proteasome for degradation. PYR41 appears to increase the accumulation of mHtt to a greater extent than MG132 treatment, suggesting that PYR41 may also inhibit the targeting of ubiquitinated mHtt to other degradation systems, such as autophagy. In fact, autophagy can also degrade ubiquitinated proteins (Shaid et al., 2013). Although whether PYR41 affects autophagy function remains to be investigated, our findings suggest that reduced degradation of misfolded mHtt accounts for the increased accumulation of mHtt in neuronal cells.

Strong evidence in support of our hypothesis is that the expression levels of E1 enzyme Ube1 are lower in brain tissues than in peripheral tissues. The lower levels of Ube1 are consistent with the increased levels of mHtt in brain tissues and *in vitro* results after inhibiting Ube1 by PYR41. The correlation between the decreased levels of Ube1 and the increased amount of ubiquitinated mHtt in the brain suggests that the high levels of Ube1 may be required for targeting the ubiquitinated proteins to the proteasome for degradation more efficiently, whereas the ubiquitination of proteins can be maintained with a low level of Ube1. The reduced levels of Ube1 in the brain also suggest that this enzyme is expressed at a lower level in neuronal cells. We should point out that the clearance of misfolded proteins by the ubiquitin-proteasome system is a complex process involving many targeting proteins. For example, there are eight E1 activating enzymes to initiate ubiquitination (Schulman and Harper, 2009) and numerous E3 ligases for substrate-specific targeting (Ardley and Robinson, 2005). It remains to be investigated whether there are tissue- or cell type-specific proteins involved in targeting mHtt to the proteasome. Also, since there are different subcellular localizations of the E1 isoforms (Grenfell et al., 1994), whether different subcellular localizations of these proteins account for the differential accumulation of mHtt in the nucleus and synapses remains to be determined. Such proteins could be additional modulators to alter the degradation of mHtt in brain regions, as well as nerve terminals and different subcellular compartments. However, the intrinsic lower levels of Ube1 in brain tissues than peripheral tissues has broad implications for the selective accumulation of misfolded proteins in the brain in a variety of neurodegenerative

diseases, including Alzheimer's and Parkinson's diseases. Furthermore, the IVDA assay we developed could be used to identify tissue-specific proteins that modulate the degradation of misfolded proteins in other polyQ and neurodegenerative diseases.

Figure 3.1

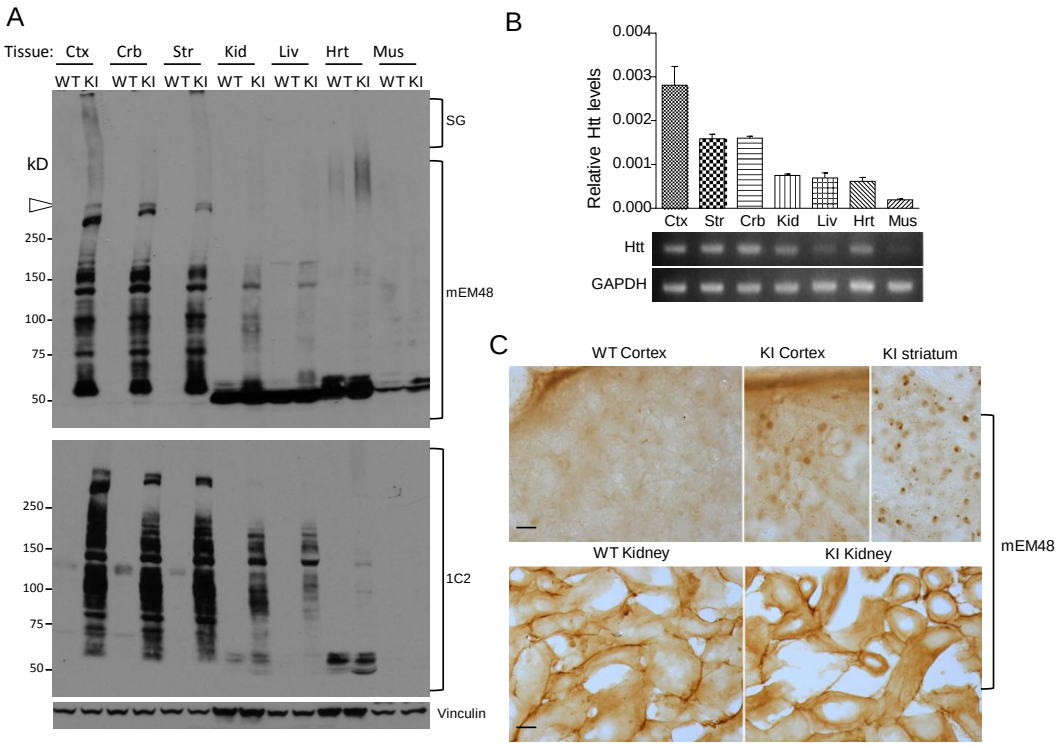
A
Tissue: Ctx Crb Str Kid Liv Hrt Mus
WT KI WT KI WT KI WT KI WT KI WT KI WT KI
kD
250
150
100
75
50
SG
mEM48
1C2
Vinculin
B
Relative Htt levels
0.004
0.003
0.002
0.001
0.000
Ctx Str Crb Kid Liv Hrt Mus
Htt
GAPDH
C
WT Cortex
KI Cortex
KI striatum
WT Kidney
KI Kidney
mEM48

Figure 3.1. Differential levels of mutant huntingtin in brain and peripheral tissues of HD CAG140 KI mice. (A) Western blotting revealing soluble full-length (open arrow head) mHtt in cortex (ctx.), striatum (str.), cerebellum (crb.), heart (hrt.), kidney (kid.), liver (liv.), and skeletal muscle (mus.). Western blots were probed with mEM48 (1:50), 1C2 (1:10,000), and anti-vinculin. WT: wild-type, KI: knock-in. SG: stacking gel. (**B**) Quantitative RT-PCR assessing the expression levels of mHtt RNA in HD CAG140 KI mice. Three brain regions and four peripheral tissues (see **A** for abbreviations) were examined. GAPDH was used as a control. The relative Htt levels were normalized by GAPDH and calculated using $R=2^{(C_{htt} - C_{gapdh})}$ (n=6). The PCR products were also analyzed by staining DNA gel (the lower panel). (**C**) Immunohistochemistry with anti-Htt (mEM48) of the cortex, striatum, and kidney tissues of 6-month-old HD KI mouse and age-matched WT mouse control. Scale bars: 10 μm.

Figure 3.2

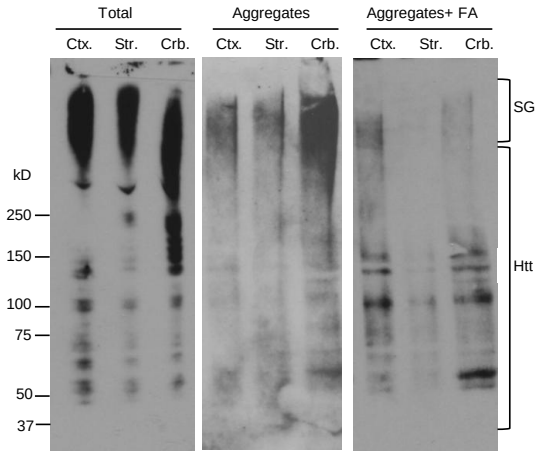
Total
Aggregates
Aggregates+ FA
Ctx.
Str.
Crb.
Ctx.
Str.
Crb.
Ctx.
Str.
Crb.
SG
kD
250
150
100
75
50
37
Htt

Figure 3.2. Formation of Htt aggregates by N-terminal mHtt fragments in HD KI mouse brain. Western blot analysis of total tissue lysates of the cortex (Ctx), striatum (Str), and cerebellum (Crb) of HD KI mouse. Different amounts of aggregated Htt were purified. Dissolving these Htt aggregates with formic acid (FA) resulted in multiple N-terminal Htt fragments that were revealed by mEM48 antibody blotting.

Figure 3.3.

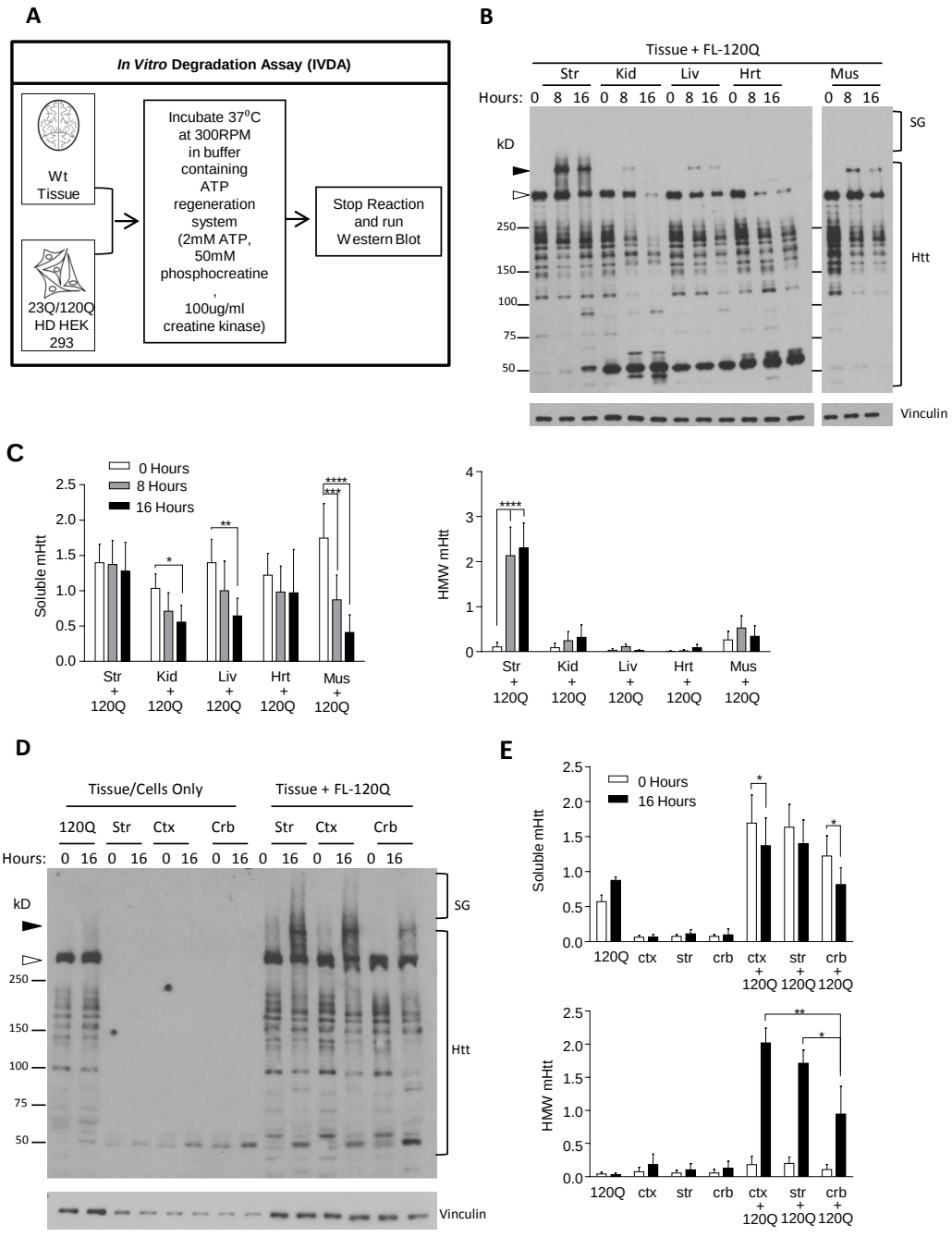
A
In Vitro Degradation Assay (IVDA)
Wt Tissue
23Q/120Q HD HEK 293
Incubate 37°C at 300RPM in buffer containing ATP regeneration system (2mM ATP, 50mM phosphocreatine, 100ug/ml creatine kinase)
Stop Reaction and run Western Blot
B
Tissue + FL-120Q
Str Kid Liv Hrt Mus
Hours: 0 8 16 0 8 16 0 8 16 0 8 16 0 8 16
kD
250
150
100
75
50
SG
Htt
Vinculin
C
0 Hours
8 Hours
16 Hours
Soluble mHtt
HMW mHtt
Str + 120Q
Kid + 120Q
Liv + 120Q
Hrt + 120Q
Mus + 120Q
D
Tissue/Cells Only
Tissue + FL-120Q
120Q Str Ctx Crb Str Ctx Crb
Hours: 0 16 0 16 0 16 0 16 0 16 0 16 0 16
kD
250
150
100
75
50
SG
Htt
Vinculin
E
0 Hours
16 Hours
Soluble mHtt
HMW mHtt
120Q ctx str crb ctx + 120Q str + 120Q crb + 120Q

Figure 3.3. In vitro degradation assay of mHtt stability. (**A**) Schematic of *in vitro* degradation assay (IVDA). (**B**) Representative western blots (mEM48 1:50) of IVDA with striatum and peripheral tissues and different brain regions at 0, 8, and 16 hours incubation. The soluble full-length mHtt is indicated by open arrowhead, and the HMW mHtt is indicated by filled arrowhead. SG is stacking gel. The cytoplasmic skeleton protein, vinculin, served as a loading control. (**C**) All soluble mHtt fragments and full-length mHtt (left panel) and HMW mHtt (right panel) were quantified as a ratio to vinculin at 0, 8, and 16 hours incubation (n=4) and normalized within the experiment to allow comparison between experiments. (**D**) Comparison of the striatum (str) with cortex (ctx) and cerebellum (crb) for their ability to process full-length mHtt by IVDA. Controls are cellular lysates only and tissue lysates only. (**E**) All soluble mHtt fragments and full-length mHtt (the upper panel) and HMW mHtt (the lower panel) in (**D**) were quantified as a ratio to vinculin and normalized. Error bars are ±SEM, statistical significance determined using repeated-measures two-way ANOVA with (Fisher's LSD test) multiple testing (* $p<0.05$, ** $p<0.01$, *** $p<0.001$, see text for exact p values).

Figure 3.4

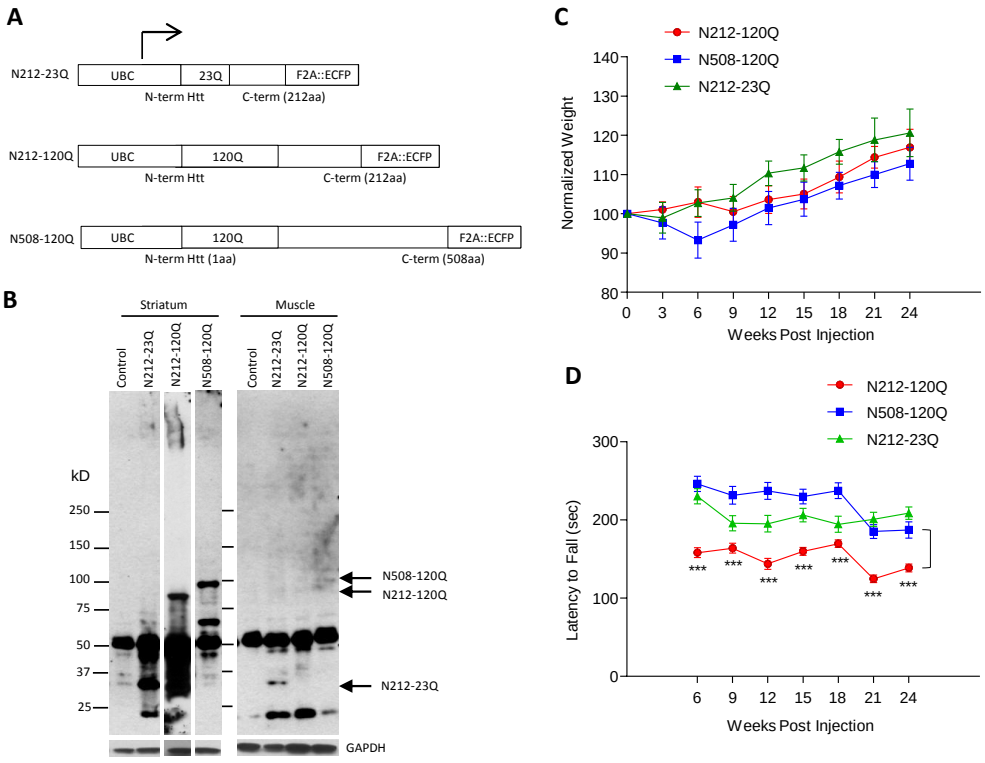
A
N212-23Q
UBC
23Q
F2A::ECFP
N-term Htt
C-term (212aa)
N212-120Q
UBC
120Q
F2A::ECFP
N-term Htt
C-term (212aa)
N508-120Q
UBC
120Q
F2A::ECFP
N-term Htt (1aa)
C-term (508aa)
B
Striatum
Muscle
Control
N212-23Q
N212-120Q
N508-120Q
kD
250
150
100
75
50
37
25
N508-120Q
N212-120Q
N212-23Q
GAPDH
C
N212-120Q
N508-120Q
N212-23Q
Normalized Weight
Weeks Post Injection
D
N212-120Q
N508-120Q
N212-23Q
Latency to Fall (sec)
Weeks Post Injection

Figure 3.4. Stability and toxicity of N-terminal mHtt fragments in vivo. (**A**) Schematic of lentiviral constructs. Htt is linked with ECFP via F2A, a peptide linker that can be self-cleaved in cells to separate mHtt from ECFP. (**B**) Western blot analysis of the striatum and muscle tissues that had been injected with lentiviral mHtt for one month. The blots were probed with mEM48 (1:50) to detect mHtt expression. (**C, D**) Body weights (C) and rotarod performance (D) of mice injected with lentiviral mHtt into their striatum were normalized to initial weight prior to surgery. Error bars are ±SEM (n=5 per group). Statistical significance determined using repeated-measures two-way ANOVA with multiple testing (Bonferroni). P value shown (*** $p<0.001$) is between N212-120Q and N508-120Q, as indicated by the bracket.

Figure 3.5

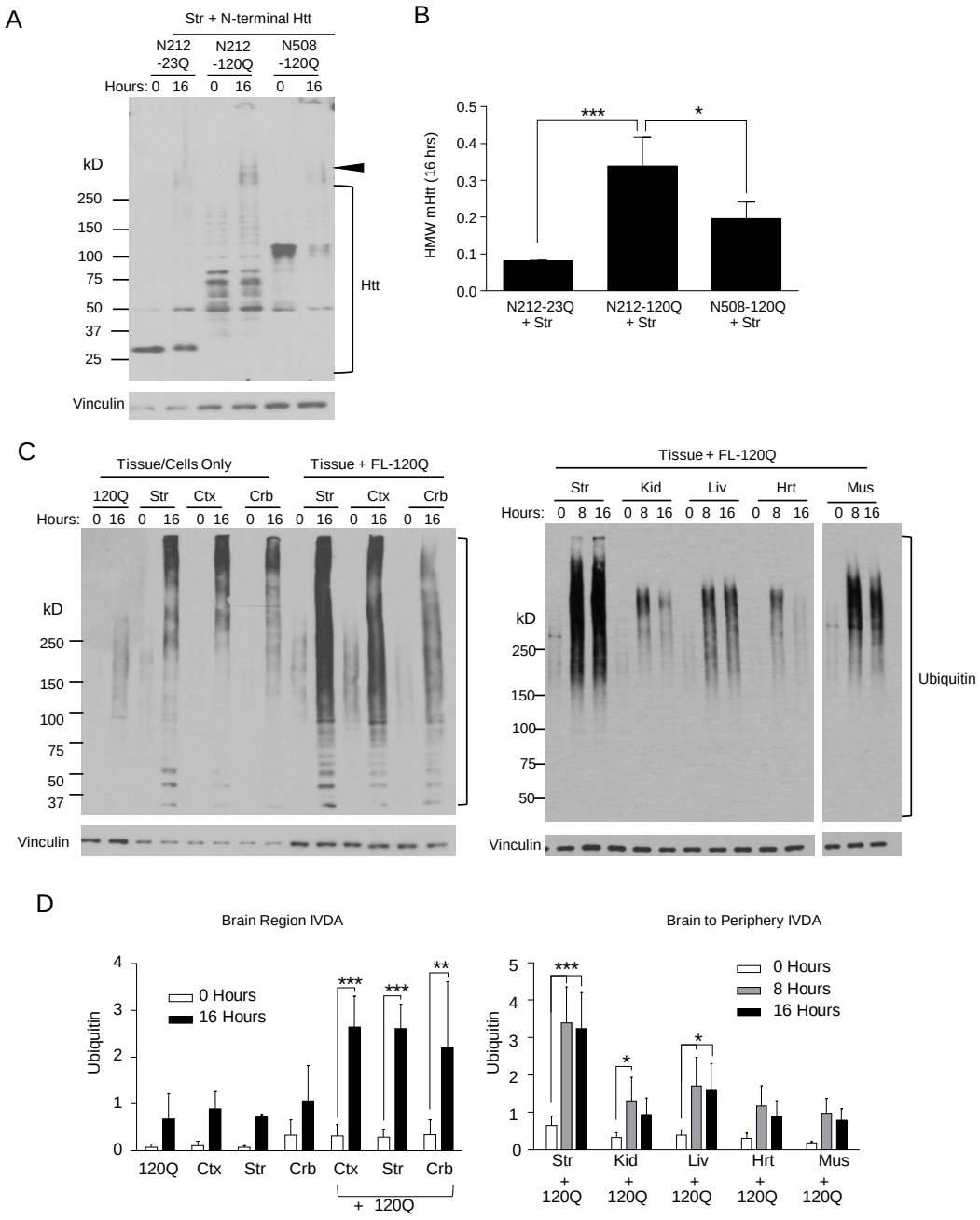
A
Str + N-terminal Htt
N212 -23Q
N212 -120Q
N508 -120Q
Hours: 0 16 0 16 0 16
kD
250
150
100
75
50
37
25
Htt
Vinculin
B
HMW mHtt (16 hrs)
0.5
0.4
0.3
0.2
0.1
0.0
***
*
N212-23Q + Str
N212-120Q + Str
N508-120Q + Str
C
Tissue/Cells Only
Tissue + FL-120Q
120Q Str Ctx Crb Str Ctx Crb
Hours: 0 16 0 16 0 16 0 16 0 16 0 16 0 16
kD
250
150
100
75
50
37
Vinculin
Tissue + FL-120Q
Str Kid Liv Hrt Mus
Hours: 0 8 16 0 8 16 0 8 16 0 8 16 0 8 16
kD
250
150
100
75
50
Ubiquitin
Vinculin
D
Brain Region IVDA
Ubiquitin
0 Hours
16 Hours
***
***
**
120Q Ctx Str Crb Ctx Str Crb
+ 120Q
Brain to Periphery IVDA
Ubiquitin
0 Hours
8 Hours
16 Hours
***
*
*
Str + 120Q
Kid + 120Q
Liv + 120Q
Hrt + 120Q
Mus + 120Q

Figure 3.5. In vitro degradation of N-terminal mHtt fragments. (**A** and **B**) N-terminal fragments of Htt (N212-23Q, N212-120Q, and N508-120Q) in transfected cell lysates were incubated with wild-type mouse striatal tissues in IVDA. Western blots (A) are shown, along with quantification of HMW mHtt (B) by two-way ANOVA with Bonferroni's multiple testing. Error bars are ±SEM (* *p<0.05,* *** *p<0.001).* (**C**) Western blot analysis of *In vitro* ubiquitination in brain and peripheral tissues. Total ubiquitin is compared among cortex, striatum, cerebellum, and peripheral tissues. Western blots are representative (n=3) of IVDA with anti-ubiquitin (P4D1 1:1000). (**D**) Quantification of total ubiquitin at 0, 8, and 16 hours incubation. Ubiquitin was quantified as a ratio to the loading control (vinculin) then normalized within the experiment. Error bars are ±SEM, statistical significance determined using repeated-measures two-way ANOVA with multiple testing (* *p<0.05,* **p<0.01,* *** *p<0.001,* see text for exact p values).

Figure 3.6

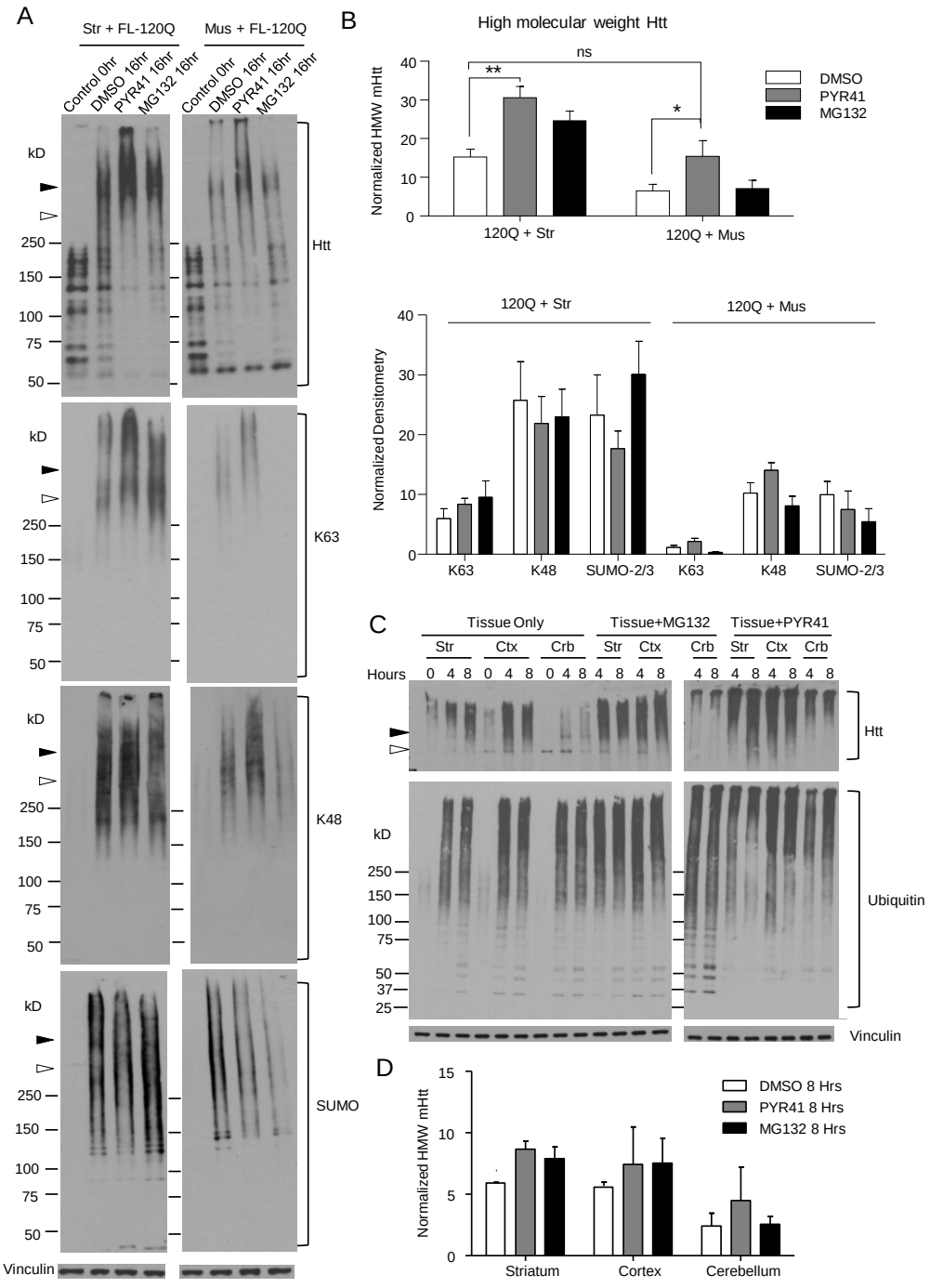
A
Str + FL-120Q
Mus + FL-120Q
Control 0hr
DMSO 16hr
PYR41 16hr
MG132 16hr
kD
250
150
100
75
50
Htt
K63
K48
SUMO
Vinculin
B
High molecular weight Htt
ns
**
*
Normalized HMW mHtt
DMSO
PYR41
MG132
120Q + Str
120Q + Mus
Normalized Densitometry
K63
K48
SUMO-2/3
C
Tissue Only
Tissue+MG132
Tissue+PYR41
Str
Ctx
Crb
Hours
0 4 8
Htt
Ubiquitin
37
25
Vinculin
D
Normalized HMW mHtt
DMSO 8 Hrs
PYR41 8 Hrs
MG132 8 Hrs
Striatum
Cortex
Cerebellum

Figure 3.6. Promotion of the formation of HMW mHtt and accumulation by inhibiting ubiquitin-activation enzyme E1. (**A**) Western blot is representative of 3 independent experiments (mEM48 1:50). Striatal tissue lysates (left panel) or muscle tissue lysates (right) were incubated with transfected full-length mHtt (FL-120Q) for 0 h and 16 h with the addition of DMSO, the E1 inhibitor PYR41 (50 μM), or the UPS inhibitor MG132 (50 μM). Open arrowhead is full-length mHtt, and filled arrowhead is mHtt oligomers. Control is the lysates before incubation. Blots were probed with (from top to bottom) antibodies to htt (mEM48), α-K63, α-K48, SUMO-2/3. (**B**) Quantification of HMW mHtt (top panel) and α-K63, α-K48, SUMO-2/3 (bottom panel) at 16 hours is shown (n=3). The ratio of HMW mHtt to vinculin was used for quantification. Error bars are ±SEM, statistical significance determined using repeated-measures two-way ANOVA with (Tukey's) multiple testing (* $p<0.05$, ** $p<0.01$). (**C**) HD KI mouse tissue lysates were incubated in vitro in IVDA buffer and treated with the E1 inhibitor PYR41 (50 μM) or the UPS inhibitor MG132 (50 μM). Western blotting showing that PYR41 or MG132 increased the accumulation of oligomerized mHtt in the cerebellar tissue compared with no drug treatment (left panel). Striatal tissue samples were also included for comparison with peripheral tissues (right panel). (**D**) Quantification of the ratio of oligomerized mHtt to vinculin after in vitro incubation at 8 h then normalized within the experiment. Error bars ±SEM (n=3).

Figure 3.7

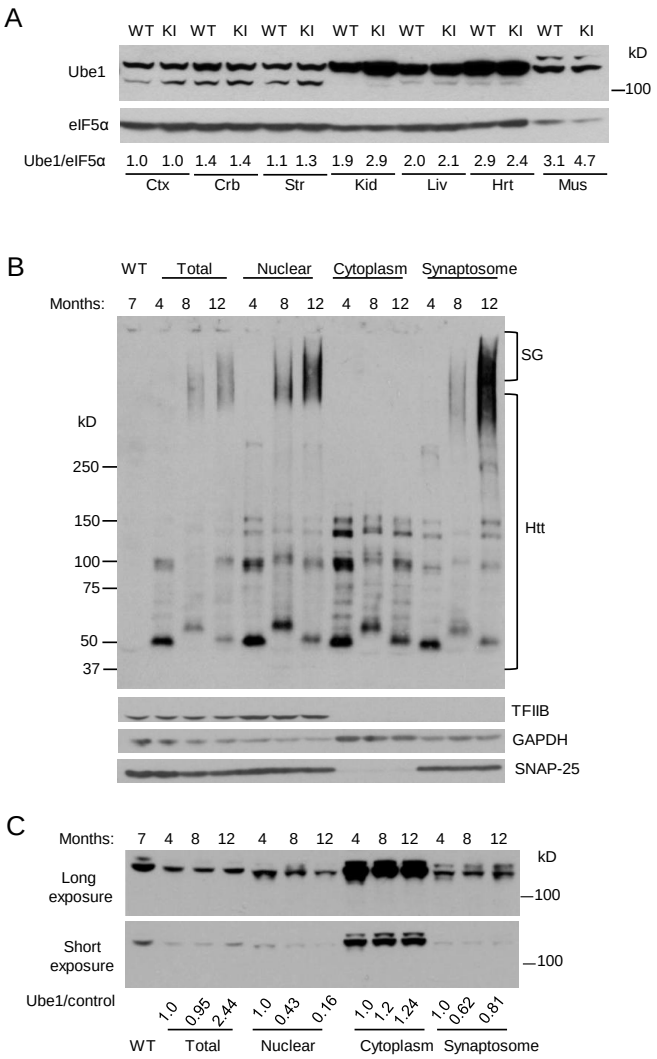
A
WT KI WT KI WT KI WT KI WT KI WT KI WT KI
kD
Ube1
100
eIF5α
Ube1/eIF5α
1.0 1.0 1.4 1.4 1.1 1.3 1.9 2.9 2.0 2.1 2.9 2.4 3.1 4.7
Ctx Crb Str Kid Liv Hrt Mus
B
WT Total Nuclear Cytoplasm Synaptosome
Months: 7 4 8 12 4 8 12 4 8 12 4 8 12
SG
kD
250
150
100
75
50
37
Htt
TFIIB
GAPDH
SNAP-25
C
Months: 7 4 8 12 4 8 12 4 8 12 4 8 12
kD
Long exposure
100
Short exposure
100
Ube1/control
1.0 0.95 2.44 1.0 0.43 0.16 1.0 1.2 1.24 1.0 0.62 0.81
WT Total Nuclear Cytoplasm Synaptosome

Figure 3.7. Differential levels of Ube1 in brain and peripheral tissues. **(A)** Western blot analysis of Ube1 in the brain and peripheral tissues of wild-type (Mangiarini et al.) and HD KI mice. The ratios of Ube1 (bottom panel) to the loading control are shown beneath the blot. (**B**) Western blot analysis of subcellular fractionations of HD KI mice at different ages. The blot was probed with anti-Htt (mEM48). The HMW mHtt increases in the nuclear and synaptosomal fractions from the aged HD KI mice. (**C**) The blot in (B) was probed with anti-Ube1, and immunoblot signals from short and long exposure times are presented. The ratios of Ube1 to that at 4 months are shown beneath the blot.

Figure 3.8

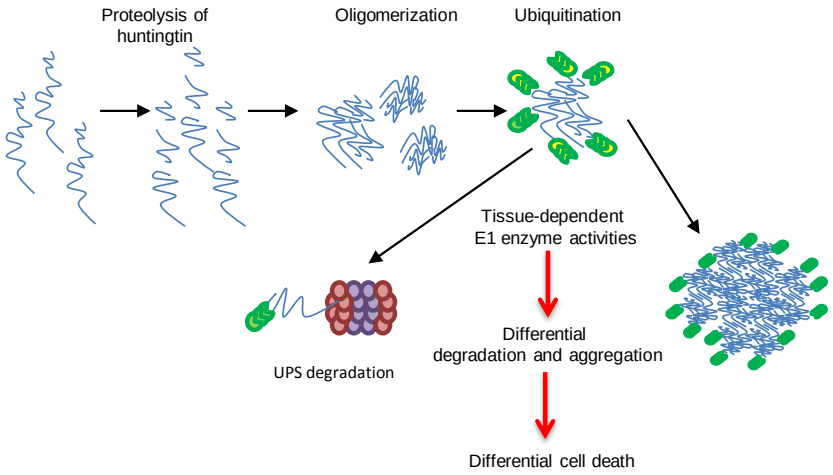
Proteolysis of huntingtin
Oligomerization
Ubiquitination
Tissue-dependent E1 enzyme activities
UPS degradation
Differential degradation and aggregation
Differential cell death

Figure 3.8. A proposed model for the differential accumulation of mHtt in affected brain regions. mHtt is cleaved to form fragments, which can form HMW mHtt and be ubiquitinated. Differential targeting of the ubiquitinated mHtt to the proteasome can lead to different levels of misfolded proteins. In striatal neurons, the reduced targeting of ubiquitinated Htt to the proteasome is likely to contribute to the preferential accumulation of mHtt in these cells, affecting the cells and forming aggregates. Ube1 activity and other targeting proteins account for the differential accumulation of mHtt in different brain regions and subcellular compartments.

Chapter 4

Conclusions and Future Directions

4.1 Summary

We have discovered a novel mechanism that contributes to the brain region specific as well as age related increase in mHtt accumulation and toxicity in Huntington's disease. We observed increased stability of mutant Htt in the brain as opposed to unaffected peripheral tissues. Increased stability of mHtt was accompanied by preferential formation of High Molecular Weight mHtt complexes (HMW mHtt) in affected brain regions (cortex and striatum) compared to unaffected brain regions (cerebellum). We also observed reduced Ubiquitin activating enzyme-1 (UBE1) in affected brain regions compared to unaffected brain regions and periphery tissues as well as a decrease in nuclear localization of UBE1 in the brain with ageing (**Figure 4.1**).

The huntingtin protein is ubiquitously expressed (Li et al., 1993; Li et al., 1995; Sharp et al., 1995; Strong et al., 1993) though the disease is characterized by neurological dysfunction and neurodegeneration that is restricted to specific regions of the brain (de la Monte et al., 1988; Vonsattel et al., 1985). We wanted to observe the expression and stability of mHtt in different tissues to learn how differences in the maintenance of mHtt transcript and protein contribute to HD. Higher levels of mHtt mRNA in the brain compared to periphery tissues suggests that mHtt expression levels contribute to Htt accumulation. Detection of mHtt protein and mRNA in several brain regions and peripheral tissues revealed more full length and fragments of mHtt protein in the brain. Dissolving aggregated mHtt allowed us to observe that aggregates in different brain regions are

composed of the same array of fragments suggesting that tissue specific factors modulate regions specific toxicity.

To observe the stability of mHtt in different tissues we developed a novel *In vitro* degradation assay (IVDA) that revealed increased stability of mHtt in the brain versus the periphery which was associated with increased accumulation of HMW mHtt in the affected brain regions compared to the unaffected regions and the periphery. These *in vitro* stability data were confirmed *in vivo* by expression of mHtt fragments into the striatum and skeletal muscle, confirming the increased stability of mHtt in the brain compared to the muscle. These data combined suggest that toxicity and the formation of mHtt aggregates are affected by the stability of mHtt protein.

Protein stability is heavily influenced by the two main cellular degradation mechanisms, autophagy and proteasome degradation. These two mechanisms are linked by ubiquitination which can target proteins to both the proteasome and for autophagy. Previous studies have shown an increase in accumulation of poly-ubiquitinated (Poly-Ub) proteins in HD mice compared to their wild-type littermates (Bennett et al., 2007) and polyQ aggregates are known to be ubiquitinated (DiFiglia et al., 1997). Though their individual roles in HD are controversial, both autophagy (Lee et al., 2012; Martinez-Vicente et al., 2010) and proteasome degradation (Bence et al., 2001; Bennett et al., 2005; Jana et al., 2001; Venkatraman et al., 2004; Wang et al., 2008a) have been shown to be disrupted in HD. Using the IVDA we were able to detect increased ubiquitination after the addition of mHtt to tissue lysates. Ubiquitination was significantly

higher in the brain than in periphery tissues. This could be interpreted in two ways: that ubiquitinated proteins are more stable in the brain, or that there is decreased degradation of ubiquitinated proteins in the brain compared to the periphery. PYR41, a drug that inhibits ubiquitination by covalently modifying the ubiquitin-activating enzyme (E1) effectively blocks the activation of ubiquitination and the subsequent addition of ubiquitin to target proteins (Yang et al., 2007). This drug allowed us to separate the effect of ubiquitination from proteasome degradation. In vitro, the striatum formed more HMW mHtt when ubiquitination was inhibited than when proteasome degradation was inhibited by MG132. Inhibition of ubiquitination in the muscle caused a significant increase in the formation of HMW mHtt. This suggests that ubiquitination is important in blocking the formation of aggregates.

In order to determine if E1 inhibition is relevant to HD we utilized tissue lysates from different brain and peripheral tissues to detect UBE1 levels. UBE1 protein is higher in peripheral tissues than brain regions and is also higher in the cerebellum than in the cortex and striatum. Importantly, there is no difference in UBE1 levels between HD and wild-type littermates, suggesting the mHtt does not inhibit the expression of UBE1. We also observed decreased levels of UBE1 in the nucleus and the synaptosome compared to the cytosolic region in HD mice, suggesting that decreased ubiquitination contributes to the increased formation of mHtt aggregates in these cellular compartments (Gutekunst et al., 1999). We also detected a decrease in UBE1 in the nucleus with age, which is consistent with the increase in mHtt nuclear inclusions in the aging brain (Li et al., 2000b).

Huntington's disease is debilitating and fatal, but treatment relies solely on modulating symptoms rather than treating the cause. My work highlights the need for a clearer understanding of the role polyQ aggregates play in HD toxicity. My work and that of others suggest two potential therapeutic targets that may prove effective. First, a drug that blocks the nuclear localization of mHtt fragments or prevents the formation of small fragments that can diffuse across the nuclear membrane. Another mechanism to achieve the same goal would be to increase the nuclear import or retention of Ube1. Ube1 phosphorylation of Serine 4 is known to influence the nuclear localization (Grenfell et al., 1994; Stephen et al., 1997), thus a drug increasing Ube1 phosphorylation could increase the nuclear Ube1 levels. This could target mHtt that entered the nucleus to the proteasome and prevent transcriptional dysregulation that is caused by nuclear accumulation of mHtt.

4.2 Remaining Questions and Future Directions

These novel findings introduce several new questions. The answer to these questions will help further define the contribution of ubiquitination, autophagy and the proteasome to HD toxicity. We have shown that ubiquitination is important for the formation of HMW mHtt and understanding its role might provide insight into the mechanism behind HD toxicity.

Does Ube1 inhibition affect autophagy?

Since autophagy is known to degrade mHtt, it is important to determine the role ubiquitin targeting plays in autophagic degradation of mHtt. The IVDA cannot account for autophagy since it is a membrane free system. To determine

how ubiquitination affects autophagy, HEK 293 cells transfected with mHtt can be treated with the ubiquitin inhibitor PYR41 and compared to cell treated with 3-MA, an inhibitor of autophagy. Treated cells can be lysed and prepared for western blotting. This can be used to detect changes in mHtt aggregation and to measure autophagic flux. In cells treated with 3-MA the LC3-II /LC3-I ratio is expected to be reduced since the conversion of LC3-I to LC3-II will be reduced. If autophagy is inhibited by PYR41 treatment then we should see a decrease in the LC3-II/ LC3-I ratio similar to what is observed in the 3-MA treated cells. If this alters aggregation of mHtt then we should see an increase in aggregations compared to control samples without drug treatment. Since ubiquitination affects multiple pathways we would expect a greater increase in aggregation with PYR41 treatment than with 3-MA treatment. To determine if there is a decrease in targeting of mHtt for autophagy these same transfected and treated cells can be used for immunofluorescent staining to detect autophagosomes. If Ube1 inhibition does decrease targeting of mHtt for autophagy then we can expect a decrease in co-localization between mHtt and autophagy associated proteins such as LC3.

Is the decrease in nuclear Ube1 a function of aging or HD?

In this work we only looked at subcellular localization of Ube1 in HD KI mice, though it is important to learn if Ube1 nuclear localization decreases with age in wild type mice as well. This is important since it may have implications for other neurodegenerative diseases. By comparing nuclear fractions from WT and HD mice at different ages we can determine if the age related decrease in nuclear

Ube1 is a function of age or if it is a result of mHtt expression. If the same decrease in nuclear localization is observed in both animals, then Ube1 localization could alter the accumulation of other disease proteins. This would be important to confirm in mouse models of other neurodegenerative disorders that involve protein accumulation. Mutation in Ube1 is known to be sufficient to reduce the lifespan of Drosophila as well as induce a neurological phenotype (Liu and Pfleger, 2013). Increasing nuclear localization of Ube1 could provide an attractive pharmaceutical target to treat a wide variety of neurodegenerative diseases. If there is no change in nuclear localization in WT mice then it is likely that mHtt alters the localization of Ube1. Using a pull down approach we could determine if mHtt aberrantly interacts with Ube1 or other proteins involved in the localization of Ube1.

What is the difference in Ube1 localization in different brain regions or cell types?

We observed higher levels of Ube1 in the periphery tissues as well as in the cerebellum compared to the brain regions most heavily affected in HD, striatum and cortex. We also observed a decrease in nuclear localization of Ube1 in HD mice with age in the cortex. Given the brain region specific nature of HD it is important to learn if there is a difference in localization of Ube1 in different brain regions. We should investigate is Ube1 localization plays a role in regional specificity of HD by performing subcellular fractionations on different regions at different ages. If we do observe a difference in the rate of decline in Ube1 nuclear localization in different tissues then this would suggest that Ube expression and

localization contribute to the regional toxicity observed in HD. If we do not observe an overt difference in Ube1 localization it could still be attributed to the initial differences observed in Ube1 protein levels.

It is also important to understand if Ube1 localization is different across cell types since it is known that neurons are more sensitive to HD toxicity than glia and it has been shown that neurons have reduced proteasome function compared to glia (Tydlacka et al., 2008). Primary cultures of glia and neurons would be prepared (Tydlacka et al., 2008) and allowed to grow to confluence in a cell culture plate. These cells could then be lysed and nuclear fractions can be collected to compare nuclear localization in glia and neurons by western blot or cells could be fixed and Ube1 localization can be detected using immunofluorescence. If there is no difference in the localization of Ube1 in these cell types, the change in localization can be observed by immunofluorescent staining of brain slices. Brain slices from animals at different ages can be double stained for Ube1 and NeuN or GFAP which are markers for neurons and glial cells, respectively. The amount of Ube1 in the nucleus can be quantified to determine if there is a cell type specific change in the localization of Ube1 with aging.

Is nuclear or cytoplasmic Ube1 localization important for htt degradation in the brain?

Mutant Htt can be found in both the cytoplasm and the nucleus where it can aberrantly interact with proteins to disrupt trafficking, transcription and other processes. Since we discovered that nuclear localization of Ube1 decreases

in the aging brain, it is important to investigate how these two populations of Ube1 affect htt half life. To achieve this goal we would first generate Ube1 constructs tagged with either a nuclear localization signal (NLS-Ube1) or a nuclear export signal (NES-Ube1) to target Ube1 to the nucleus or the cytoplasm. We would transfect 293 HEK cells that stably express full length mHtt with these Ube1 constructs in order to measure mHtt half life measured by mHtt protein levels by western blotting. If nuclear Ube1 is more important for mHtt half life we would expect to see a greater increase in mHtt degradation in the cells transfected with NLS-Ube1 compared to those with NES-Ube1. If, instead, cytoplasmic Ube1 is more important for mHtt stability we would expect to see a greater decrease in mHtt levels in the NES-Ube1 transfected cells. We could also measure the affect of Ube1 localization on the formation of aggregates using subcellular fractionation to observe aggregate formation in the cytoplasm and the nucleus in cells transfected with the NLS or NES-Ube1. If nuclear stability of mHtt is more important for the formation of mHtt aggregates we would expect to see a decrease in nuclear aggregates in the NLS-Ube1 transfected cells.

Does Ube6 contribute to Huntington's disease toxicity?

Until recently Ube1 was the only one of 8 identified E1 enzymes shown to interact with ubiquitin (Schulman and Harper, 2009) though Ube6 has recently been identified as a second E1 activating enzyme to interact with Ub (Jin et al., 2007) while no other E1's have been shown to interact with ubiquitin. It is unclear whether PYR41 can inhibit the activity of all E1's or just Ube1. It is important to determine if Ube6 can be affected by PYR41 and if it plays any role

in HD. To determine if PYR41 acts on Ube6 we could utilize an *in vitro* ubiquitination assay. First we would transfect HEK 293 cells with FLAG-Ube6. Ube6 must be detected using the FLAG tag since reliable antibodies for this protein have not been generated. After over-expressing FLAG-Ube6 we would purify the protein from cell lysates and treat it with PYR41 in the presence of purified ubiquitin. If Ube6 is affected by PYR41 we would expect to see a dose dependent decrease in the Ube6-ubiqutin complex by running the samples on a non denaturing PAGE gel. If we do see a decrease in the Ube6-Ub complex then PYR41 can inhibit the activity of Ube6 as well as Ube1, suggesting that Ube6 inhibition could also affect mHtt aggregation.

To determine if Ube6 affects mHtt aggregation I propose testing if over expression of either Ube1 or Ube6 can decrease formation of HMW mHtt in the IVDA. First we would transfect HEK 293 cells that stably express FL mHtt with FLAG-Ube6, FLAG-Ube1 or a control plasmid. The cells would then be lysed and mixed with striatal tissue lysate from a WT animal. These samples should be treated with PYR41. If Ube1 or Ube6 over expression can reduce the formation of HMW mHtt in the presence of PYR41 then this links their activity directly to the formation of HMW mHtt. If Ube6 cannot rescue HMW mHtt formation then Ube6 ubiquitination does not affect mHtt aggregation. If it can rescue HMW mHtt formation then Ube6 ubiquitination does alter mHtt aggregation and the role of Ube6 should be explored further.

4.3 Conclusions

Huntington's disease is a debilitating and fatal neurodegenerative disease. The mechanisms contributing to HD toxicity are not well understood. The work presented in this dissertation identifies a novel factor that plays a role in the brain region specific as well as age related increase in mHtt accumulation and toxicity in Huntington's disease. First, mHtt is more stable in the brain than in unaffected peripheral tissues. Second, mHtt preferentially forms HMW mHtt in affected brain regions compared to unaffected brain regions and the periphery. Thirdly, Ube1 is reduced in affected brain regions compared to unaffected tissues and Ube1 nuclear localization decreases in the brain with ageing. These observations provide a better understanding of the brain region and age related toxicity that characterizes Huntington's disease.

Figure 4.1

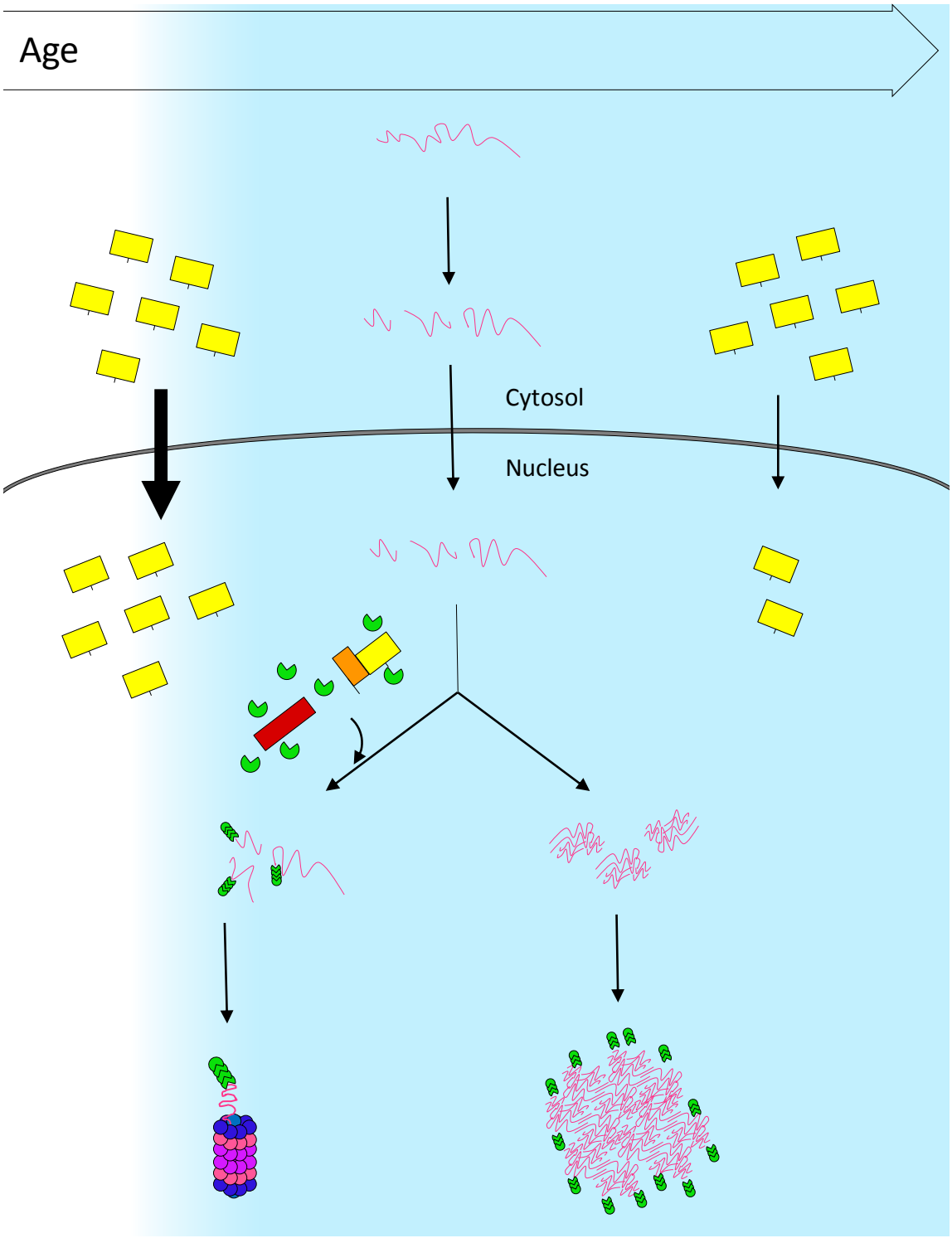

Figure 4.1. A model for the age dependent decline in nuclear localization of Ube1 and its effect on mHtt aggregation. (Center) Full length mHtt is cleaved into fragments by proteases. These fragments can enter the nucleus. In young neurons (left) Ube1 (yellow) is localized in the nucleus, promoting the ubiquitination of soluble mHtt fragments and their subsequent degradation by the proteasome. In aged neurons (right) nuclear Ube1 is reduced. Soluble mHtt fragments form oligomers and form large insoluble aggregates which can be ubiquitinated. Ageing is represented by a blue gradient from left to right.

References

Andrade, M.A., and Bork, P. (1995). HEAT repeats in the Huntington's disease protein. Nat Genet *11*, 115-116.

Ardley, H.C., and Robinson, P.A. (2005). E3 ubiquitin ligases. Essays Biochem *41*, 15-30.

Bence, N.F., Sampat, R.M., and Kopito, R.R. (2001). Impairment of the ubiquitin-proteasome system by protein aggregation. Science *292*, 1552-1555.

Bennett, E.J., Bence, N.F., Jayakumar, R., and Kopito, R.R. (2005). Global impairment of the ubiquitin-proteasome system by nuclear or cytoplasmic protein aggregates precedes inclusion body formation. Mol Cell *17*, 351-365.

Bennett, E.J., Shaler, T.A., Woodman, B., Ryu, K.Y., Zaitseva, T.S., Becker, C.H., Bates, G.P., Schulman, H., and Kopito, R.R. (2007). Global changes to the ubiquitin system in Huntington's disease. Nature *448*, 704-708.

Bett, J.S., Cook, C., Petrucelli, L., and Bates, G.P. (2009). The ubiquitin-proteasome reporter GFPu does not accumulate in neurons of the R6/2 transgenic mouse model of Huntington's disease. PLoS One *4*, e5128.

Bhat, K.P., Yan, S., Wang, C.E., Li, S., and Li, X.J. (2014). Differential ubiquitination and degradation of huntingtin fragments modulated by ubiquitin-protein ligase E3A. Proc Natl Acad Sci U S A *111*, 5706-5711.

Chau, V., Tobias, J.W., Bachmair, A., Marriott, D., Ecker, D.J., Gonda, D.K., and Varshavsky, A. (1989). A multiubiquitin chain is confined to specific lysine in a targeted short-lived protein. Science *243*, 1576-1583.

Cooper, J.K., Schilling, G., Peters, M.F., Herring, W.J., Sharp, A.H., Kaminsky, Z., Masone, J., Khan, F.A., Delanoy, M., Borchelt, D.R.*, et al.* (1998). Truncated N-terminal fragments of huntingtin with expanded glutamine repeats form nuclear and cytoplasmic aggregates in cell culture. Hum Mol Genet *7*, 783-790.

Cornett, J., Cao, F., Wang, C.E., Ross, C.A., Bates, G.P., Li, S.H., and Li, X.J. (2005). Polyglutamine expansion of huntingtin impairs its nuclear export. Nat Genet *37*, 198-204.

Davies, S.W., Turmaine, M., Cozens, B.A., DiFiglia, M., Sharp, A.H., Ross, C.A., Scherzinger, E., Wanker, E.E., Mangiarini, L., and Bates, G.P. (1997). Formation of neuronal intranuclear inclusions underlies the neurological dysfunction in mice transgenic for the HD mutation. Cell *90*, 537-548.

de la Monte, S.M., Vonsattel, J.P., and Richardson, E.P., Jr. (1988). Morphometric demonstration of atrophic changes in the cerebral cortex, white

matter, and neostriatum in Huntington's disease. Journal of neuropathology and experimental neurology *47*, 516-525.

Diaz-Hernandez, M., Hernandez, F., Martin-Aparicio, E., Gomez-Ramos, P., Moran, M.A., Castano, J.G., Ferrer, I., Avila, J., and Lucas, J.J. (2003). Neuronal induction of the immunoproteasome in Huntington's disease. J Neurosci *23*, 11653-11661.

DiFiglia, M., Sapp, E., Chase, K.O., Davies, S.W., Bates, G.P., Vonsattel, J.P., and Aronin, N. (1997). Aggregation of huntingtin in neuronal intranuclear inclusions and dystrophic neurites in brain. Science *277*, 1990-1993.

Driver-Dunckley E, C.J. (2007). Huntington's Disease. In: Schapira AHV. Neurology and Clinical Neuroscience. , Vol 67 (Elsevier).

Dunah, A.W., Jeong, H., Griffin, A., Kim, Y.M., Standaert, D.G., Hersch, S.M., Mouradian, M.M., Young, A.B., Tanese, N., and Krainc, D. (2002). Sp1 and TAFII130 transcriptional activity disrupted in early Huntington's disease. Science *296*, 2238-2243.

Duyao, M., Ambrose, C., Myers, R., Novelletto, A., Persichetti, F., Frontali, M., Folstein, S., Ross, C., Franz, M., Abbott, M., *et al.* (1993). Trinucleotide repeat length instability and age of onset in Huntington's disease. Nat Genet *4*, 387-392.

Duyao, M.P., Auerbach, A.B., Ryan, A., Persichetti, F., Barnes, G.T., McNeil, S.M., Ge, P., Vonsattel, J.P., Gusella, J.F., Joyner, A.L.*, et al.* (1995). Inactivation of the mouse Huntington's disease gene homolog Hdh. Science *269*, 407-410.

Friedman, M.J., Shah, A.G., Fang, Z.H., Ward, E.G., Warren, S.T., Li, S., and Li, X.J. (2007). Polyglutamine domain modulates the TBP-TFIIB interaction: implications for its normal function and neurodegeneration. Nat Neurosci *10*, 1519-1528.

Fusco, F.R., Chen, Q., Lamoreaux, W.J., Figueredo-Cardenas, G., Jiao, Y., Coffman, J.A., Surmeier, D.J., Honig, M.G., Carlock, L.R., and Reiner, A. (1999). Cellular localization of huntingtin in striatal and cortical neurons in rats: lack of correlation with neuronal vulnerability in Huntington's disease. J Neurosci *19*, 1189-1202.

Gafni, J., and Ellerby, L.M. (2002). Calpain activation in Huntington's disease. J Neurosci *22*, 4842-4849.

Gafni, J., Hermel, E., Young, J.E., Wellington, C.L., Hayden, M.R., and Ellerby, L.M. (2004). Inhibition of calpain cleavage of huntingtin reduces toxicity: accumulation of calpain/caspase fragments in the nucleus. J Biol Chem *279*, 20211-20220.

Gauthier, L.R., Charrin, B.C., Borrell-Pages, M., Dompierre, J.P., Rangone, H., Cordelieres, F.P., De Mey, J., MacDonald, M.E., Lessmann, V., Humbert, S.*, et al.* (2004). Huntingtin controls neurotrophic support and survival of neurons by enhancing BDNF vesicular transport along microtubules. Cell *118*, 127-138.

Goldstein, G., Scheid, M., Hammerling, U., Schlesinger, D.H., Niall, H.D., and Boyse, E.A. (1975). Isolation of a polypeptide that has lymphocyte-differentiating properties and is probably represented universally in living cells. Proc Natl Acad Sci U S A *72*, 11-15.

Gong, B., Kielar, C., and Morton, A.J. (2012). Temporal separation of aggregation and ubiquitination during early inclusion formation in transgenic mice carrying the Huntington's disease mutation. PLoS One *7*, e41450.

Gray, M., Shirasaki, D.I., Cepeda, C., Andre, V.M., Wilburn, B., Lu, X.H., Tao, J., Yamazaki, I., Li, S.H., Sun, Y.E.*, et al.* (2008). Full-length human mutant huntingtin with a stable polyglutamine repeat can elicit progressive and selective neuropathogenesis in BACHD mice. J Neurosci *28*, 6182-6195.

Grenfell, S.J., Trausch-Azar, J.S., Handley-Gearhart, P.M., Ciechanover, A., and Schwartz, A.L. (1994). Nuclear localization of the ubiquitin-activating enzyme, E1, is cell-cycle-dependent. Biochem J *300 (Pt 3)*, 701-708.

Group, H.s.D.C.R. (1993). A novel gene containing a trinucleotide repeat that is expanded and unstable on Huntington's disease chromosomes. . Cell *72*, 971-983.

Gutekunst, C.A., Li, S.H., Yi, H., Mulroy, J.S., Kuemmerle, S., Jones, R., Rye, D., Ferrante, R.J., Hersch, S.M., and Li, X.J. (1999). Nuclear and neuropil aggregates in Huntington's disease: relationship to neuropathology. J Neurosci *19*, 2522-2534.

Haacke, A., Hartl, F.U., and Breuer, P. (2007). Calpain inhibition is sufficient to suppress aggregation of polyglutamine-expanded ataxin-3. J Biol Chem *282*, 18851-18856.

Hackam, A.S., Singaraja, R., Wellington, C.L., Metzler, M., McCutcheon, K., Zhang, T., Kalchman, M., and Hayden, M.R. (1998). The influence of huntingtin protein size on nuclear localization and cellular toxicity. J Cell Biol *141*, 1097-1105.

Hara, T., Nakamura, K., Matsui, M., Yamamoto, A., Nakahara, Y., Suzuki-Migishima, R., Yokoyama, M., Mishima, K., Saito, I., Okano, H.*, et al.* (2006). Suppression of basal autophagy in neural cells causes neurodegenerative disease in mice. Nature *441*, 885-889.

Harper, P.S. (1992). The epidemiology of Huntington's disease. Hum Genet *89*, 365-376.

Havel, L.S., Wang, C.E., Wade, B., Huang, B., Li, S., and Li, X.J. (2011). Preferential accumulation of N-terminal mutant huntingtin in the nuclei of striatal neurons is regulated by phosphorylation. Hum Mol Genet *20*, 1424-1437.

Heng, M.Y., Detloff, P.J., and Albin, R.L. (2008). Rodent genetic models of Huntington disease. Neurobiol Dis *32*, 1-9.

Hickey, M.A., Kosmalska, A., Enayati, J., Cohen, R., Zeitlin, S., Levine, M.S., and Chesselet, M.F. (2008). Extensive early motor and non-motor behavioral deficits are followed by striatal neuronal loss in knock-in Huntington's disease mice. Neuroscience *157*, 280-295.

Hodgson, J.G., Agopyan, N., Gutekunst, C.A., Leavitt, B.R., LePiane, F., Singaraja, R., Smith, D.J., Bissada, N., McCutcheon, K., Nasir, J.*, et al.* (1999). A YAC mouse model for Huntington's disease with full-length mutant huntingtin, cytoplasmic toxicity, and selective striatal neurodegeneration. Neuron *23*, 181-192.

Jana, N.R., Zemskov, E.A., Wang, G., and Nukina, N. (2001). Altered proteasomal function due to the expression of polyglutamine-expanded truncated N-terminal huntingtin induces apoptosis by caspase activation through mitochondrial cytochrome c release. Hum Mol Genet *10*, 1049-1059.

Jin, J., Li, X., Gygi, S.P., and Harper, J.W. (2007). Dual E1 activation systems for ubiquitin differentially regulate E2 enzyme charging. Nature *447*, 1135-1138.

Kalchman, M.A., Graham, R.K., Xia, G., Koide, H.B., Hodgson, J.G., Graham, K.C., Goldberg, Y.P., Gietz, R.D., Pickart, C.M., and Hayden, M.R. (1996). Huntingtin is ubiquitinated and interacts with a specific ubiquitin-conjugating enzyme. J Biol Chem *271*, 19385-19394.

Kazemi-Esfarjani, P., and Benzer, S. (2000). Genetic suppression of polyglutamine toxicity in Drosophila. Science *287*, 1837-1840.

Kerscher, O., Felberbaum, R., and Hochstrasser, M. (2006). Modification of proteins by ubiquitin and ubiquitin-like proteins. Annu Rev Cell Dev Biol *22*, 159-180.

Kim, Y.J., Yi, Y., Sapp, E., Wang, Y., Cuiffo, B., Kegel, K.B., Qin, Z.H., Aronin, N., and DiFiglia, M. (2001). Caspase 3-cleaved N-terminal fragments of wild-type and mutant huntingtin are present in normal and Huntington's disease brains, associate with membranes, and undergo calpain-dependent proteolysis. Proc Natl Acad Sci U S A *98*, 12784-12789.

Komatsu, M., Waguri, S., Chiba, T., Murata, S., Iwata, J., Tanida, I., Ueno, T., Koike, M., Uchiyama, Y., Kominami, E.*, et al.* (2006). Loss of autophagy in the central nervous system causes neurodegeneration in mice. Nature *441*, 880-884.

Kuemmerle, S., Gutekunst, C.A., Klein, A.M., Li, X.J., Li, S.H., Beal, M.F., Hersch, S.M., and Ferrante, R.J. (1999). Huntington aggregates may not predict neuronal death in Huntington's disease. Ann Neurol *46*, 842-849.

La Spada, A.R., Wilson, E.M., Lubahn, D.B., Harding, A.E., and Fischbeck, K.H. (1991). Androgen receptor gene mutations in X-linked spinal and bulbar muscular atrophy. Nature *352*, 77-79.

Landles, C., and Bates, G.P. (2004). Huntingtin and the molecular pathogenesis of Huntington's disease. Fourth in molecular medicine review series. EMBO Rep *5*, 958-963.

Landles, C., Sathasivam, K., Weiss, A., Woodman, B., Moffitt, H., Finkbeiner, S., Sun, B., Gafni, J., Ellerby, L.M., Trottier, Y.*, et al.* (2010). Proteolysis of mutant huntingtin produces an exon 1 fragment that accumulates as an aggregated protein in neuronal nuclei in Huntington disease. J Biol Chem *285*, 8808-8823.

Lee, H., Noh, J.Y., Oh, Y., Kim, Y., Chang, J.W., Chung, C.W., Lee, S.T., Kim, M., Ryu, H., and Jung, Y.K. (2012). IRE1 plays an essential role in ER stress-mediated aggregation of mutant huntingtin via the inhibition of autophagy flux. Hum Mol Genet *21*, 101-114.

Legleiter, J., Mitchell, E., Lotz, G.P., Sapp, E., Ng, C., DiFiglia, M., Thompson, L.M., and Muchowski, P.J. (2010). Mutant huntingtin fragments form oligomers

in a polyglutamine length-dependent manner in vitro and in vivo. J Biol Chem *285*, 14777-14790.

Li, H., Li, S.H., Cheng, A.L., Mangiarini, L., Bates, G.P., and Li, X.J. (1999). Ultrastructural localization and progressive formation of neuropil aggregates in Huntington's disease transgenic mice. Hum Mol Genet *8*, 1227-1236.

Li, H., Li, S.H., Johnston, H., Shelbourne, P.F., and Li, X.J. (2000a). Amino-terminal fragments of mutant huntingtin show selective accumulation in striatal neurons and synaptic toxicity. Nat Genet *25*, 385-389.

Li, H., Li, S.H., Yu, Z.X., Shelbourne, P., and Li, X.J. (2001). Huntingtin aggregate-associated axonal degeneration is an early pathological event in Huntington's disease mice. J Neurosci *21*, 8473-8481.

Li, S.H., Gutekunst, C.A., Hersch, S.M., and Li, X.J. (1998). Interaction of huntingtin-associated protein with dynactin P150Glued. The Journal of neuroscience : the official journal of the Society for Neuroscience *18*, 1261-1269.

Li, S.H., Li, H., Torre, E.R., and Li, X.J. (2000b). Expression of huntingtin-associated protein-1 in neuronal cells implicates a role in neuritic growth. Mol Cell Neurosci *16*, 168-183.

Li, S.H., and Li, X.J. (1998). Aggregation of N-terminal huntingtin is dependent on the length of its glutamine repeats. Hum Mol Genet *7*, 777-782.

Li, S.H., and Li, X.J. (2004). Huntingtin and its role in neuronal degeneration. Neuroscientist *10*, 467-475.

Li, S.H., Schilling, G., Young, W.S., 3rd, Li, X.J., Margolis, R.L., Stine, O.C., Wagster, M.V., Abbott, M.H., Franz, M.L., Ranen, N.G., *et al.* (1993). Huntington's disease gene (IT15) is widely expressed in human and rat tissues. Neuron *11*, 985-993.

Li, W., Serpell, L.C., Carter, W.J., Rubinsztein, D.C., and Huntington, J.A. (2006). Expression and characterization of full-length human huntingtin, an elongated HEAT repeat protein. J Biol Chem *281*, 15916-15922.

Li, X., Wang, C.E., Huang, S., Xu, X., Li, X.J., Li, H., and Li, S. (2010). Inhibiting the ubiquitin-proteasome system leads to preferential accumulation of toxic N-terminal mutant huntingtin fragments. Hum Mol Genet *19*, 2445-2455.

Li, X.J., and Li, S. (2011). Proteasomal dysfunction in aging and Huntington disease. Neurobiol Dis *43*, 4-8.

Li, X.J., Li, S.H., Sharp, A.H., Nucifora, F.C., Jr., Schilling, G., Lanahan, A., Worley, P., Snyder, S.H., and Ross, C.A. (1995). A huntingtin-associated protein enriched in brain with implications for pathology. Nature *378*, 398-402.

Lim, K.L., and Lim, G.G. (2011). K63-linked ubiquitination and neurodegeneration. Neurobiol Dis *43*, 9-16.

Lin, C.H., Tallaksen-Greene, S., Chien, W.M., Cearley, J.A., Jackson, W.S., Crouse, A.B., Ren, S., Li, X.J., Albin, R.L., and Detloff, P.J. (2001). Neurological abnormalities in a knock-in mouse model of Huntington's disease. Hum Mol Genet *10*, 137-144.

Liu, C., Fei, E., Jia, N., Wang, H., Tao, R., Iwata, A., Nukina, N., Zhou, J., and Wang, G. (2007). Assembly of lysine 63-linked ubiquitin conjugates by phosphorylated alpha-synuclein implies Lewy body biogenesis. J Biol Chem *282*, 14558-14566.

Liu, H.Y., and Pfleger, C.M. (2013). Mutation in E1, the ubiquitin activating enzyme, reduces Drosophila lifespan and results in motor impairment. PLoS One *8*, e32835.

Lotz, G.P., Legleiter, J., Aron, R., Mitchell, E.J., Huang, S.Y., Ng, C., Glabe, C., Thompson, L.M., and Muchowski, P.J. (2010). Hsp70 and Hsp40 functionally

interact with soluble mutant huntingtin oligomers in a classic ATP-dependent reaction cycle. J Biol Chem *285*, 38183-38193.

Lunkes, A., Lindenberg, K.S., Ben-Haiem, L., Weber, C., Devys, D., Landwehrmeyer, G.B., Mandel, J.L., and Trottier, Y. (2002). Proteases acting on mutant huntingtin generate cleaved products that differentially build up cytoplasmic and nuclear inclusions. Mol Cell *10*, 259-269.

Mangiarini, L., Sathasivam, K., Seller, M., Cozens, B., Harper, A., Hetherington, C., Lawton, M., Trottier, Y., Lehrach, H., Davies, S.W.*, et al.* (1996). Exon 1 of the HD gene with an expanded CAG repeat is sufficient to cause a progressive neurological phenotype in transgenic mice. Cell *87*, 493-506.

Mao, Y., Senic-Matuglia, F., Di Fiore, P.P., Polo, S., Hodsdon, M.E., and De Camilli, P. (2005). Deubiquitinating function of ataxin-3: insights from the solution structure of the Josephin domain. Proc Natl Acad Sci U S A *102*, 12700-12705.

Marcellin, D., Abramowski, D., Young, D., Richter, J., Weiss, A., Marcel, A., Maassen, J., Kauffmann, M., Bibel, M., Shimshek, D.R.*, et al.* (2012). Fragments of HdhQ150 mutant huntingtin form a soluble oligomer pool that declines with aggregate deposition upon aging. PLoS One *7*, e44457.

Martin, J.B., and Gusella, J.F. (1986). Huntington's disease. Pathogenesis and management. N Engl J Med *315*, 1267-1276.

Martinez-Vicente, M., Talloczy, Z., Wong, E., Tang, G., Koga, H., Kaushik, S., de Vries, R., Arias, E., Harris, S., Sulzer, D.*, et al.* (2010). Cargo recognition failure is responsible for inefficient autophagy in Huntington's disease. Nat Neurosci *13*, 567-576.

Maynard, C.J., Bottcher, C., Ortega, Z., Smith, R., Florea, B.I., Diaz-Hernandez, M., Brundin, P., Overkleeft, H.S., Li, J.Y., Lucas, J.J.*, et al.* (2009). Accumulation of ubiquitin conjugates in a polyglutamine disease model occurs without global ubiquitin/proteasome system impairment. Proc Natl Acad Sci U S A *106*, 13986-13991.

McGuire, J.R., Rong, J., Li, S.H., and Li, X.J. (2006). Interaction of Huntingtin-associated protein-1 with kinesin light chain: implications in intracellular trafficking in neurons. The Journal of biological chemistry *281*, 3552-3559.

Menalled, L.B., Sison, J.D., Dragatsis, I., Zeitlin, S., and Chesselet, M.F. (2003). Time course of early motor and neuropathological anomalies in a knock-in mouse model of Huntington's disease with 140 CAG repeats. J Comp Neurol *465*, 11-26.

Miller, J.P., Holcomb, J., Al-Ramahi, I., de Haro, M., Gafni, J., Zhang, N., Kim, E., Sanhueza, M., Torcassi, C., Kwak, S.*, et al.* (2010). Matrix metalloproteinases

are modifiers of huntingtin proteolysis and toxicity in Huntington's disease. Neuron *67*, 199-212.

Mitra, S., Tsvetkov, A.S., and Finkbeiner, S. (2009). Single neuron ubiquitin-proteasome dynamics accompanying inclusion body formation in huntington disease. J Biol Chem *284*, 4398-4403.

Nance, M.A., and Myers, R.H. (2001). Juvenile onset Huntington's disease--clinical and research perspectives. Mental retardation and developmental disabilities research reviews *7*, 153-157.

Nasir, J., Floresco, S.B., O'Kusky, J.R., Diewert, V.M., Richman, J.M., Zeisler, J., Borowski, A., Marth, J.D., Phillips, A.G., and Hayden, M.R. (1995). Targeted disruption of the Huntington's disease gene results in embryonic lethality and behavioral and morphological changes in heterozygotes. Cell *81*, 811-823.

Ordway, J.M., Tallaksen-Greene, S., Gutekunst, C.A., Bernstein, E.M., Cearley, J.A., Wiener, H.W., Dure, L.S.t., Lindsey, R., Hersch, S.M., Jope, R.S.*, et al.* (1997). Ectopically expressed CAG repeats cause intranuclear inclusions and a progressive late onset neurological phenotype in the mouse. Cell *91*, 753-763.

Ortega, Z., Diaz-Hernandez, M., Maynard, C.J., Hernandez, F., Dantuma, N.P., and Lucas, J.J. (2010). Acute polyglutamine expression in inducible mouse

model unravels ubiquitin/proteasome system impairment and permanent recovery attributable to aggregate formation. J Neurosci *30*, 3675-3688.

Palhan, V.B., Chen, S., Peng, G.H., Tjernberg, A., Gamper, A.M., Fan, Y., Chait, B.T., La Spada, A.R., and Roeder, R.G. (2005). Polyglutamine-expanded ataxin-7 inhibits STAGA histone acetyltransferase activity to produce retinal degeneration. Proc Natl Acad Sci U S A *102*, 8472-8477.

Perutz, M. (1994). Polar zippers: their role in human disease. Protein science : a publication of the Protein Society *3*, 1629-1637.

Perutz, M.F. (1995). Glutamine repeats as polar zippers: their role in inherited neurodegenerative disease. Molecular medicine *1*, 718-721.

Poirier, M.A., Li, H., Macosko, J., Cai, S., Amzel, M., and Ross, C.A. (2002). Huntingtin spheroids and protofibrils as precursors in polyglutamine fibrilization. J Biol Chem *277*, 41032-41037.

Ralser, M., Albrecht, M., Nonhoff, U., Lengauer, T., Lehrach, H., and Krobitsch, S. (2005). An integrative approach to gain insights into the cellular function of human ataxin-2. J Mol Biol *346*, 203-214.

Ratovitski, T., Nakamura, M., D'Ambola, J., Chighladze, E., Liang, Y., Wang, W., Graham, R., Hayden, M.R., Borchelt, D.R., Hirschhorn, R.R.*, et al.* (2007). N-

terminal proteolysis of full-length mutant huntingtin in an inducible PC12 cell model of Huntington's disease. Cell Cycle *6*, 2970-2981.

Ravikumar, B., Duden, R., and Rubinsztein, D.C. (2002). Aggregate-prone proteins with polyglutamine and polyalanine expansions are degraded by autophagy. Hum Mol Genet *11*, 1107-1117.

Ravikumar, B., Vacher, C., Berger, Z., Davies, J.E., Luo, S., Oroz, L.G., Scaravilli, F., Easton, D.F., Duden, R., O'Kane, C.J.*, et al.* (2004). Inhibition of mTOR induces autophagy and reduces toxicity of polyglutamine expansions in fly and mouse models of Huntington disease. Nat Genet *36*, 585-595.

Sathasivam, K., Lane, A., Legleiter, J., Warley, A., Woodman, B., Finkbeiner, S., Paganetti, P., Muchowski, P.J., Wilson, S., and Bates, G.P. (2010). Identical oligomeric and fibrillar structures captured from the brains of R6/2 and knock-in mouse models of Huntington's disease. Hum Mol Genet *19*, 65-78.

Sathasivam, K., Neueder, A., Gipson, T.A., Landles, C., Benjamin, A.C., Bondulich, M.K., Smith, D.L., Faull, R.L., Roos, R.A., Howland, D.*, et al.* (2013). Aberrant splicing of HTT generates the pathogenic exon 1 protein in Huntington disease. Proc Natl Acad Sci U S A *110*, 2366-2370.

Saudou, F., Finkbeiner, S., Devys, D., and Greenberg, M.E. (1998). Huntingtin acts in the nucleus to induce apoptosis but death does not correlate with the formation of intranuclear inclusions. Cell *95*, 55-66.

Scherzinger, E., Lurz, R., Turmaine, M., Mangiarini, L., Hollenbach, B., Hasenbank, R., Bates, G.P., Davies, S.W., Lehrach, H., and Wanker, E.E. (1997). Huntingtin-encoded polyglutamine expansions form amyloid-like protein aggregates in vitro and in vivo. Cell *90*, 549-558.

Schilling, G., Becher, M.W., Sharp, A.H., Jinnah, H.A., Duan, K., Kotzuk, J.A., Slunt, H.H., Ratovitski, T., Cooper, J.K., Jenkins, N.A.*, et al.* (1999a). Intranuclear inclusions and neuritic aggregates in transgenic mice expressing a mutant N-terminal fragment of huntingtin. Hum Mol Genet *8*, 397-407.

Schilling, G., Wood, J.D., Duan, K., Slunt, H.H., Gonzales, V., Yamada, M., Cooper, J.K., Margolis, R.L., Jenkins, N.A., Copeland, N.G.*, et al.* (1999b). Nuclear accumulation of truncated atrophin-1 fragments in a transgenic mouse model of DRPLA. Neuron *24*, 275-286.

Schulman, B.A., and Harper, J.W. (2009). Ubiquitin-like protein activation by E1 enzymes: the apex for downstream signalling pathways. Nat Rev Mol Cell Biol *10*, 319-331.

Shaid, S., Brandts, C.H., Serve, H., and Dikic, I. (2013). Ubiquitination and selective autophagy. Cell death and differentiation *20*, 21-30.

Sharp, A.H., Loev, S.J., Schilling, G., Li, S.H., Li, X.J., Bao, J., Wagster, M.V., Kotzuk, J.A., Steiner, J.P., Lo, A.*, et al.* (1995). Widespread expression of Huntington's disease gene (IT15) protein product. Neuron *14*, 1065-1074.

Shibata, M., Lu, T., Furuya, T., Degterev, A., Mizushima, N., Yoshimori, T., MacDonald, M., Yankner, B., and Yuan, J. (2006). Regulation of intracellular accumulation of mutant Huntingtin by Beclin 1. J Biol Chem *281*, 14474-14485.

Si, K., Das, K., and Maitra, U. (1996). Characterization of multiple mRNAs that encode mammalian translation initiation factor 5 (eIF-5). J Biol Chem *271*, 16934-16938.

Slow, E.J., van Raamsdonk, J., Rogers, D., Coleman, S.H., Graham, R.K., Deng, Y., Oh, R., Bissada, N., Hossain, S.M., Yang, Y.Z.*, et al.* (2003). Selective striatal neuronal loss in a YAC128 mouse model of Huntington disease. Hum Mol Genet *12*, 1555-1567.

Steffan, J.S., Agrawal, N., Pallos, J., Rockabrand, E., Trotman, L.C., Slepko, N., Illes, K., Lukacsovich, T., Zhu, Y.Z., Cattaneo, E.*, et al.* (2004). SUMO modification of Huntingtin and Huntington's disease pathology. Science *304*, 100-104.

Stephen, A.G., Trausch-Azar, J.S., Handley-Gearhart, P.M., Ciechanover, A., and Schwartz, A.L. (1997). Identification of a region within the ubiquitin-activating enzyme required for nuclear targeting and phosphorylation. J Biol Chem *272*, 10895-10903.

Strong, T.V., Tagle, D.A., Valdes, J.M., Elmer, L.W., Boehm, K., Swaroop, M., Kaatz, K.W., Collins, F.S., and Albin, R.L. (1993). Widespread expression of the human and rat Huntington's disease gene in brain and nonneural tissues. Nat Genet *5*, 259-265.

Tan, J.M., Wong, E.S., Kirkpatrick, D.S., Pletnikova, O., Ko, H.S., Tay, S.P., Ho, M.W., Troncoso, J., Gygi, S.P., Lee, M.K.*, et al.* (2008). Lysine 63-linked ubiquitination promotes the formation and autophagic clearance of protein inclusions associated with neurodegenerative diseases. Hum Mol Genet *17*, 431-439.

Tonoki, A., Kuranaga, E., Tomioka, T., Hamazaki, J., Murata, S., Tanaka, K., and Miura, M. (2009). Genetic evidence linking age-dependent attenuation of the 26S proteasome with the aging process. Molecular and cellular biology *29*, 1095-1106.

Tsai, C.C., Kao, H.Y., Mitzutani, A., Banayo, E., Rajan, H., McKeown, M., and Evans, R.M. (2004). Ataxin 1, a SCA1 neurodegenerative disorder protein, is functionally linked to the silencing mediator of retinoid and thyroid hormone receptors. Proc Natl Acad Sci U S A *101*, 4047-4052.

Tydlacka, S., Wang, C.E., Wang, X., Li, S., and Li, X.J. (2008). Differential activities of the ubiquitin-proteasome system in neurons versus glia may account for the preferential accumulation of misfolded proteins in neurons. J Neurosci *28*, 13285-13295.

Venkatraman, P., Wetzel, R., Tanaka, M., Nukina, N., and Goldberg, A.L. (2004). Eukaryotic proteasomes cannot digest polyglutamine sequences and release them during degradation of polyglutamine-containing proteins. Mol Cell *14*, 95-104.

Vonsattel, J.P., Myers, R.H., Stevens, T.J., Ferrante, R.J., Bird, E.D., and Richardson, E.P., Jr. (1985). Neuropathological classification of Huntington's disease. Journal of neuropathology and experimental neurology *44*, 559-577.

Wacker, J.L., Zareie, M.H., Fong, H., Sarikaya, M., and Muchowski, P.J. (2004). Hsp70 and Hsp40 attenuate formation of spherical and annular polyglutamine oligomers by partitioning monomer. Nat Struct Mol Biol *11*, 1215-1222.

Wang, C.E., Tydlacka, S., Orr, A.L., Yang, S.H., Graham, R.K., Hayden, M.R., Li, S., Chan, A.W., and Li, X.J. (2008a). Accumulation of N-terminal mutant huntingtin in mouse and monkey models implicated as a pathogenic mechanism in Huntington's disease. Hum Mol Genet *17*, 2738-2751.

Wang, J., Wang, C.E., Orr, A., Tydlacka, S., Li, S.H., and Li, X.J. (2008b). Impaired ubiquitin-proteasome system activity in the synapses of Huntington's disease mice. J Cell Biol *180*, 1177-1189.

Warrick, J.M., Chan, H.Y., Gray-Board, G.L., Chai, Y., Paulson, H.L., and Bonini, N.M. (1999). Suppression of polyglutamine-mediated neurodegeneration in Drosophila by the molecular chaperone HSP70. Nat Genet *23*, 425-428.

Weiss, A., Trager, U., Wild, E.J., Grueninger, S., Farmer, R., Landles, C., Scahill, R.I., Lahiri, N., Haider, S., Macdonald, D.*, et al.* (2012). Mutant huntingtin fragmentation in immune cells tracks Huntington's disease progression. J Clin Invest *122*, 3731-3736.

Wellington, C.L., Ellerby, L.M., Gutekunst, C.A., Rogers, D., Warby, S., Graham, R.K., Loubser, O., van Raamsdonk, J., Singaraja, R., Yang, Y.Z.*, et al.* (2002). Caspase cleavage of mutant huntingtin precedes neurodegeneration in Huntington's disease. J Neurosci *22*, 7862-7872.

Wellington, C.L., Ellerby, L.M., Hackam, A.S., Margolis, R.L., Trifiro, M.A., Singaraja, R., McCutcheon, K., Salvesen, G.S., Propp, S.S., Bromm, M.*, et al.* (1998). Caspase cleavage of gene products associated with triplet expansion disorders generates truncated fragments containing the polyglutamine tract. J Biol Chem *273*, 9158-9167.

Wellington, C.L., Singaraja, R., Ellerby, L., Savill, J., Roy, S., Leavitt, B., Cattaneo, E., Hackam, A., Sharp, A., Thornberry, N.*, et al.* (2000). Inhibiting caspase cleavage of huntingtin reduces toxicity and aggregate formation in neuronal and nonneuronal cells. J Biol Chem *275*, 19831-19838.

Wood, J.D., Nucifora, F.C., Jr., Duan, K., Zhang, C., Wang, J., Kim, Y., Schilling, G., Sacchi, N., Liu, J.M., and Ross, C.A. (2000). Atrophin-1, the dentato-rubral and pallido-luysian atrophy gene product, interacts with ETO/MTG8 in the nuclear matrix and represses transcription. J Cell Biol *150*, 939-948.

Xu, Q., Huang, S., Song, M., Wang, C.E., Yan, S., Liu, X., Gaertig, M.A., Yu, S.P., Li, H., Li, S.*, et al.* (2013). Synaptic mutant huntingtin inhibits synapsin-1 phosphorylation and causes neurological symptoms. J Cell Biol *202*, 1123-1138.

Yang, Y., Kitagaki, J., Dai, R.M., Tsai, Y.C., Lorick, K.L., Ludwig, R.L., Pierre, S.A., Jensen, J.P., Davydov, I.V., Oberoi, P.*, et al.* (2007). Inhibitors of ubiquitin-activating enzyme (E1), a new class of potential cancer therapeutics. Cancer Res *67*, 9472-9481.

Zeitlin, S., Liu, J.P., Chapman, D.L., Papaioannou, V.E., and Efstratiadis, A. (1995). Increased apoptosis and early embryonic lethality in mice nullizygous for the Huntington's disease gene homologue. Nature genetics *11*, 155-163.

Zhou, H., Cao, F., Wang, Z., Yu, Z.X., Nguyen, H.P., Evans, J., Li, S.H., and Li, X.J. (2003). Huntingtin forms toxic NH2-terminal fragment complexes that are promoted by the age-dependent decrease in proteasome activity. J Cell Biol *163*, 109-118.

Zhuchenko, O., Bailey, J., Bonnen, P., Ashizawa, T., Stockton, D.W., Amos, C., Dobyns, W.B., Subramony, S.H., Zoghbi, H.Y., and Lee, C.C. (1997). Autosomal dominant cerebellar ataxia (SCA6) associated with small polyglutamine expansions in the alpha 1A-voltage-dependent calcium channel. Nat Genet *15*, 62-69.

Zuccato, C., Ciammola, A., Rigamonti, D., Leavitt, B.R., Goffredo, D., Conti, L., MacDonald, M.E., Friedlander, R.M., Silani, V., Hayden, M.R.*, et al.* (2001). Loss of huntingtin-mediated BDNF gene transcription in Huntington's disease. Science *293*, 493-498.

Zuccato, C., Tartari, M., Crotti, A., Goffredo, D., Valenza, M., Conti, L., Cataudella, T., Leavitt, B.R., Hayden, M.R., Timmusk, T.*, et al.* (2003). Huntingtin interacts with REST/NRSF to modulate the transcription of NRSE-controlled neuronal genes. Nat Genet *35*, 76-83.